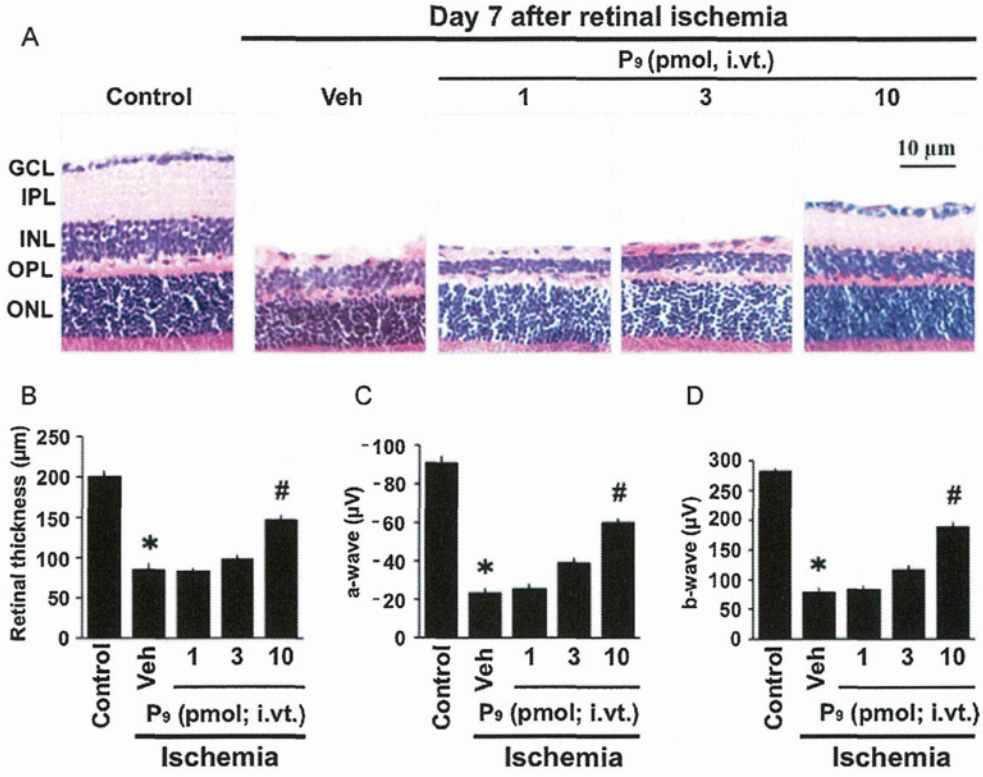

Fig. 2. P_9 peptide inhibits retinal ischemic damages. P_9 is injected intravitreously (i.vt.) with doses of 1, 3 and 10 pmol/μl in the ipsilateral eye at 24 h after retinal ischemia. Vehicle is treated with 0.05% DMSO in a similar manner. (A–D) Dose-dependent protective activity of P_9 against ischemic damages. (A) H&E staining of retinal section is performed in control (left panel), vehicle (middle panel) and P_9 post-treated mice (right panel) at day 7 after retinal ischemia. (B–D) Measurement of retinal thickness (B) as well as the a-wave (C) and b-wave (D) amplitudes of ERG analysis are performed at day 7 after retinal ischemia in control, vehicle and P_9 post-treated mice. The median effective dose of P_9 is 8 pmol/eye for a-wave ($n = 10$), and 4 pmol/eye for b-wave ($n = 10$) of ERG analysis. Data are mean ± S.E.M. ($^*P < 0.05$, *vs.* control, $^\#P < 0.05$, *vs.* Veh) from experiments using 5–7 mice for each group.

3.2. P_9-induced recovery of retinal ischemic damages

To examine whether P_9 has *in vivo* protective effect against ischemic damages, P_9 was injected intravitreously (i.vt.) in the ipsilateral eye with doses of 1, 3 and 10 pmol/μl at 24 h after retinal ischemia. The hematoxylin and eosin (H&E) staining data revealed that number of cells in different retinal layers and retinal thickness are significantly decreased in the vehicle-treated mice at day 7 after ischemia, whereas 10 pmol P_9, but not 1 and 3 pmol maximally and significantly blocked the cellular loss and decrease in retinal thickness at day 7, compared to vehicle (Fig. 2A and B). The a- and b-wave amplitudes in electroretinogram (ERG) study represent the functional activity of photoreceptor cells in the outer nuclear layer (ONL), and mixture of cells in different retinal layers including bipolar, amacrine, Muller and ganglion cells, respectively [13,17]. Experiments using ERG analysis showed that a- and b-wave amplitudes are significantly decreased in the vehicle-treated mice at day 7 after retinal ischemia, compared to control (Fig. 2C and D). Following P_9 injection, amplitudes of a- and b-waves were gradually increased in a dose-dependent manner and 10 pmol P_9 induced the maximum protective effect against ischemic damages at day 7 after ischemia, compared to vehicle (Fig. 2C and D). The a-wave value for naive (non-ischemia) was 94 ± 6 μV ($n = 7$), while 22 ± 3 μV ($n = 7$) for vehicle (ischemia alone). Thus, the median effective dose for P_9 to give 50 μV was 8 pmol/eye. On the other hand, b-wave values for naive (non-ischemia) and vehicle (ischemia alone) were 292 ± 8 μV ($n = 7$) and 90 ± 4 μV ($n = 7$), respectively. In the case of b-wave, the median effective dose for P_9 to give 150 μV was 4 pmol/eye.

3.3. P_9 ameliorates the cerebral ischemic brain

To evaluate the P_9-induced protection against the ischemic damages in brain, P_9 was intravenously (i.v.) administered with doses of 0.1, 0.3 and 1 mg/kg at 1 h after cerebral ischemia (1 h tMCAO), and subsequent 2,3,5-triphenyl tetrazolium chloride (TTC) staining and behavioral tests were performed at 24 h after the ischemic stress. The infarct volume was calculated as the percentage of damaged areas in the ischemic brain on the ipsilateral side to the contralateral side. TTC staining data showed that cerebral ischemia causes a significant increase in ipsilateral infarct volume in the vehicle-treated ischemic mice to 51 ± 3% ($n = 7$) of control. Following systemic injection of P_9 (1 mg/kg, i.v.), infarct volume was maximally and significantly decreased at 24 h in the ischemic brain treated with 0.3 or 1 mg/kg of P_9, which had been given at 1 h after the ischemic stress (33 ± 3%, $n = 7$, and 30 ± 2%, $n = 7$, respectively), compared to vehicle (Fig. 3A and B). On the other hand, the behavioral study showed that clinical scores are significantly increased at 24 h after ischemia in vehicle-treated mice (score: 3.5 ± 0.5, $n = 6$) (Fig. 3C). The systemic injection (i.v.) with 0.3 or 1 mg of P_9 at 1 h after tMCAO caused the significant decline in clinical scores (scores: 2.5 ± 0.5, $n = 6$, and 2.0 ± 0.5, $n = 7$, respectively), as shown in Fig. 3C.

3.4. Blockade of cerebral ischemia-induced blood vessel damages by P_9

To investigate whether P_9 inhibits the ischemia-induced blood vessel damages, P_9 was injected (1 mg/kg, i.v.) at 1 h after cerebral

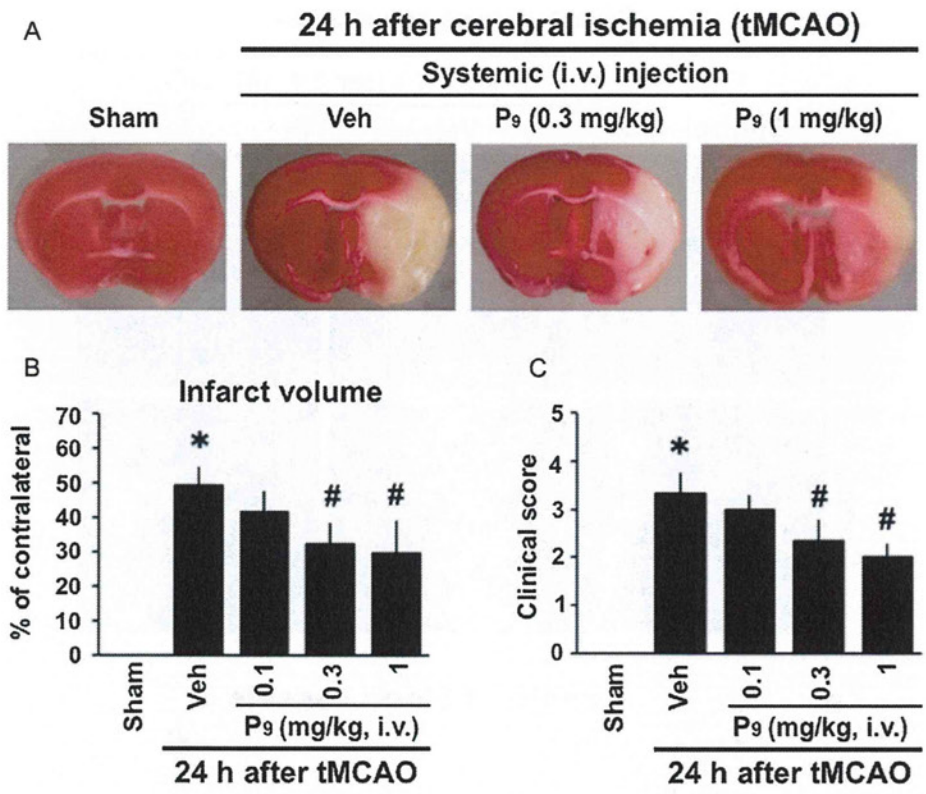

Fig. 3. P_9 improves cerebral ischemic brain. P_9 is injected intravenously (i.v.) with doses of 0.1, 0.3 and 1 mg/kg at 1 h after cerebral ischemia (1 h tMCAO). Vehicles are treated with equal volume of K^+-free PBS in a similar manner. (A–C) TTC staining (A), measurement of infarct volume (B) and clinical scores (C) are performed in sham-operated, vehicle-treated and P_9-treated mice at 24 h after tMCAO. Data represent the means ± S.E.M. ($^*P < 0.05$, *vs.* Sham, $^\#P < 0.05$, *vs.* Veh). Experiments are performed using 5–7 mice for each group.

ischemia (1 h tMCAO). Following *in vivo* binding with biotinylated tomato lectin, the damages of blood vessels after fixation were evaluated by staining with Alexa Fluor 488 streptavidin at day 1 after tMCAO. When the damage was calculated as the ratio of averaged length of blood vessels in the region of somatosensory cortex on the ipsilateral side to the contralateral side, the cerebral ischemia caused a significant decrease to 45 ± 5% ($n = 6$) of control. The systemic injection of P_9 (1 mg/kg, i.v.) completely prevented the ischemia-induced damages of blood vessels (108 ± 6%, $n = 7$), as shown in Fig. 4A and B. Similar significant prevention by P_9 was observed in the striatum (control: 100%, $n = 6$; ischemia alone: 47 ± 4%, $n = 6$; ischemia + P_9: 104 ± 3%, $n = 7$) and hippocampus (control: 100%, $n = 6$; ischemia alone: 34 ± 5%, $n = 6$; ischemia + P_9: 102 ± 4%, $n = 7$).

4. Discussion

The present study includes the following important findings: (1) the 9-amino acid peptide P_9 (amino acids 52–60) derived from ProTα shows the full survival activity in cultured neuronal cells against ischemic stress, (2) P_9 significantly ameliorates the ischemic damages in retina and brain, and (3) P_9 prevents the cerebral ischemia-induced disruption of blood vessels.

The previous *in vitro* investigations suggested that the action of ProTα is related to cell survival [6,23,24,30,45,47], though the sequence-specific diverse functions of ProTα also have been reported [5,14,15,36,42,43]. Most recently, we demonstrated using various deletion mutants of GST-ProTα that the active core peptide P_{30} (amino acids 49–78), but not N-terminal (amino acids 2–29) including the sequence (amino acids 1–48) or C-terminal sequence (amino acids 79–112 and 102–112) in ProTα induces original survival effect in cultured cortical neurons against the ischemic stress [17]. In the present study, we firstly applied alanine scanning technique for the determination of minimum peptide sequence of P_{30} that exerts full neuroprotective effect in cultured cortical neurons under ischemic (serum-free) condition. The findings revealed that the replacement of amino acids D50 and N51 with alanine (D50A and N51A) retains the original survival activity of P_{30} in cortical neurons against the ischemic stress, whereas alanine replacement of E52, V53, and E55 (E52A, V53A, and E55A) exerted partial survival action. Interestingly, the neuroprotective effect of P_{30} was significantly abolished when replaced amino acids between E56 and G60 by alanine. However, the peptide comprised of 54–73 amino acid residues as well as the C-terminal sequence of P_{30} (amino acids 59–78) induced no neuroprotective action against ischemic stress. Therefore, our *in vitro* study clarified that this 9-amino acid peptide P_9 (amino acids 52–60) represents the short active core sequence in P_{30}, which is required for full-length neuroprotection.

Next, we performed *in vivo* experiments to examine the neuroprotective effect of P_9 against ischemic stress in retina and brain. Retinal ischemia is associated with injury-related mechanism-induced destruction of cellular and functional response in the different cell layers of retina, leading to visual disorders and blindness [31,32]. Since retinal ischemic model provides higher reproducibility to comprehend the pathophysiological alternation and signaling cascades [37], this ischemic stress was used as a simple model for screening the neuroprotective action of P_9 by intravitreous administration. It is evident that ProTα improves the ischemic damages in retina [13,47,50]. Most recently, our *in vivo* study demonstrated that P_{30} peptide in ProTα inhibits

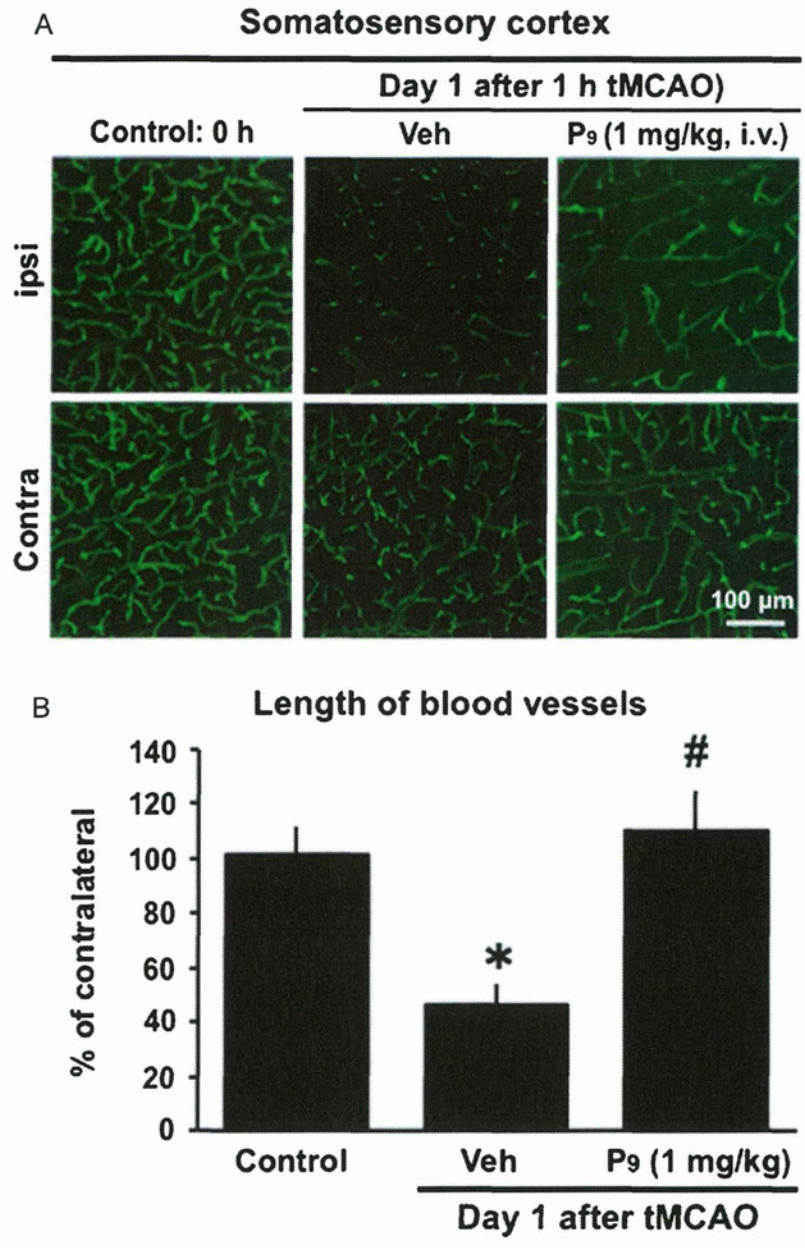

Fig. 4. P_9 prevents cerebral ischemia-induced blood vessel disruption. P_9 is administered (1 mg/kg, i.v.) at 1 h after cerebral ischemia (1 h tMCAO). (A and B) Following biotinylated tomato lectin injection (1 mg/ml, 100 μl, i.v.) at 24 h after tMCAO, and subsequent perfusion of mice 5 min after tomato lectin delivery, the staining of blood vessels using Alexa Fluor 488 streptavidin (A) as well as measurement of the length of blood vessels (B) is performed at day 1 after the ischemic stress. Data represent the means ± S.E.M. ($^*P < 0.05$, *vs.* control, $^\#P < 0.05$, *vs.* Veh) from experiments using 5–7 mice for each group.

ischemia-induced retinal damages [17]. The present findings using H&E staining and ERG analysis revealed that intravitreous treatment with 10 pmol of P_9 at 24 h after retinal ischemia markedly rescues the ischemia-induced decrease in retinal thickness and cell number in different layers in the retina.

Brain ischemia is one of the major clinical issue that is associated with irreversible neurological damages, along with dysfunction of motor, sensory and cognitive systems [10,20,39,40]. There are several reports about ProTα-induced blockade of ischemic brain damages [12,17,48]. Following cerebral ischemia (tMCAO), in the present study, the experiments using TTC staining and behavioral assessment in terms of clinical score suggested that systemic administration of P_9 (1 mg/kg, i.v.) at 1 h after tMCAO significantly improves the ischemic brain. Ischemic stress in the brain causes adequate breakdown of blood vessels [2,19], whereas this disruption of blood vessels is protected by P_{30} peptide [17]. The experiment of fluorescence staining by *in vivo* tomato lectin administration showed the P_9-induced (1 mg/kg, i.v.) significant prevention of ischemia-induced cerebral blood vessel damages at day 1.

It is interesting to examine the potency ratio of P_9-induced protection to P_{30}, which has recently been reported. In the present retinal ischemia model, the median effective dose of P_9 to give 50 μV was approximately 8 pmol/eye for a-wave, and to give 150 μV was 4 pmol/eye for b-wave of ERG analysis, respectively, while these values for P_{30} were 2 and 1 pmol/eye, respectively [17],

indicating that P_9 is 4 times less potent than P_{30}. In the cerebral ischemia model, on the other hand, systemic treatment (i.v.) with 0.3 or 1 mg/kg of P_{30} causes markedly decrease in infarct volume at 24 h after the ischemic stress ($33 \pm 3\%$ and $30 \pm 2\%$, respectively), compared to ischemia alone ($52 \pm 3\%$), suggesting that the value with 0.3 mg/kg (approximately 0.3 μmol/kg) of P_9 is equivalent to that with 0.3 mg/kg (~0.1 μmol/kg) of P_{30}. Regarding the clinical score, the value (score: 2.0 ± 0.5) with 1 mg/kg (~1.0 μmol/kg) of P_9 is equivalent to that (score: 2.0 ± 0.5) with 1 mg/kg (~0.3 μmol/kg) of P_{30} [17] indicating that P_9 is 3 times less potent than P_{30} in cerebral ischemia-induced infarction and clinical score. All together, it is evident that the relative potencies of P_9 to P_{30} in prevention of retinal and brain damages seem to be similar, though the administration routes are different (local/intravitreous and systemic/intravenous, respectively). Cerebral ischemic stress disrupts the blood–brain barrier (BBB) [26,35], but we previously found that ProTα through intraperitoneal (i.p.) route is penetrated into the damaged regions in cerebral and retinal ischemia models [12,13]. It is considered that smaller peptides are generally preferable in BBB-penetration, while at the same time they are more susceptible to enzymatic degradation [22,38]. Thus, similar relative potency of P_9 and P_{30} in the present study may be a result of these opposite factors. The present study suggests that P_9 would be a promising prototype of small peptides to prevent the stroke. However, much more detailed studies should be performed prior to the future studies of peptide modification. They include (1) the quantitative beneficial actions in cultured neuronal cell death, and its mechanisms, (2) different administration schedules *in vivo*, (3) assessment studies of BBB-penetration and metabolic stability. All these studies are in progress in our group.

In conclusion, ProTα-derived 9-amino acid peptide P_9 induced potent actions against the cerebral and retinal ischemic damages. Thus, the present study would be a key demonstration to develop a new type of peptidic medicines against stroke.

Conflict of interest

Authors have no conflict interest to report.

Acknowledgments

We thank R. Fujita, H. Yamaguchi and S. Maeda for technical assistance and advice. We also thank M. Moskowitz for the valuable discussion. We acknowledge parts of this study were supported by Grants-in-Aid for Scientific Research (to H.U.) from the Ministry of Education, Culture, Sports, Science and Technology (MEXT) and Health and Labor Sciences Research Grants (to H.U.) on Research from the Ministry of Health, Labor and Welfare.

References

[1] Abdelmohsen K, Lal A, Kim HH, Gorospe M. Posttranscriptional orchestration of an anti-apoptotic program by HuR. Cell Cycle 2007;6:1288–92.
[2] Beck H, Plate KH. Angiogenesis after cerebral ischemia. Acta Neuropathol 2009;117:481–96.
[3] Bejot Y, Prigent-Tessier A, Cachia C, Giroud M, Mossiat C, Bertrand N, et al. Time-dependent contribution of non neuronal cells to BDNF production after ischemic stroke in rats. Neurochem Int 2011;58:102–11.
[4] Blanco RE, Soto I, Duprey-Díaz M, Blagburn. Upregulation of brain-derived neurotrophic factor by application of fibroblast growth factor-2 to the cut optic nerve is important for long term survival of retinal ganglion cells. J Neurosci Res 2008;86:3382–92.
[5] Danielli R, Fonsatti E, Calabrò L, Giacomo AM, Maio M. Thymosin α1 in melanoma: from the clinical trial setting to the daily practice and beyond. Ann NY Acad Sci 2012;1270:8–12.
[6] Dong G, Callegari EA, Gloeckner CJ, Ueffing M, Wang H. Prothymosin-α interacts with mutant huntingtin and suppresses its cytotoxicity in cell culture. J Biol Chem 2012;287:1279–89.
[7] Dvoriantchikova G, Barakat DJ, Hernandez E, Shestopalov VI, Ivanov D. Liposome-delivered ATP effectively protects the retina against ischemia-reperfusion injury. Mol Vis 2010;16:2882–90.
[8] Feigin VL. Stroke epidemiology in the developing world. Lancet 2005;365:2160–1.
[9] Flynn RW, MacWalter RS, Doney AS. The cost of cerebral ischaemia. Neuropharmacology 2008;55:250–6.
[10] Fornage M. Genetics of stroke. Curr Atheroscler Rep 2009;11:167–74.
[11] Fujita R, Ueda H. Protein kinase C-mediated necrosis-apoptosis switch of cortical neurons by conditioned medium factors secreted under the serum-free stress. Cell Death Differ 2003;10:782–90.
[12] Fujita R, Ueda H. Prothymosin-alpha1 prevents necrosis and apoptosis following stroke. Cell Death Differ 2007;14:1839–42.
[13] Fujita R, Ueda M, Fujiwara K, Ueda H. Prothymosin-alpha plays a defensive role in retinal ischemia through necrosis and apoptosis inhibition. Cell Death Differ 2009;16:349–58.
[14] Garaci E, Favalli C, Pica F, Sinibaldi Vallebona P, Palamara AT, Matteucci C, et al. Thymosin alpha 1: from bench to bedside. Ann NY Acad Sci 2007;1112:225–34.
[15] Goldstein AL, Goldstein AL. From lab to bedside: emerging clinical applications of thymosin alpha 1. Expert Opin Biol Ther 2009;9:593–608.
[16] Halder SK, Matsunaga H, Ueda H. Neuron-specific non-classical release of prothymosin alpha, a novel neuroprotective DAMPs. J Neurochem 2012;123:262–75.
[17] Halder SK, Matsunaga H, Yamaguchi H, Ueda H. Novel neuroprotective action of prothymosin alpha-derived peptide against retinal and brain ischemic damages. J Neurochem 2013, http://dx.doi.org/10.1111/jnc.12132.
[18] Hancock R, Bertrand HC, Tsujita T, Naz S, El-Bakry A, Laoruchupong J, et al. Peptide inhibitors of the Keap1–Nrf2 protein–protein interaction. Free Radic Biol Med 2012;52:444–51.
[19] Haqqani AS, Nesic M, Preston E, Baumann E, Kelly J, Stanimirovic D. Characterization of vascular protein expression patterns in cerebral ischemia/reperfusion using laser capture microdissection and ICAT-nanoLC–MS/MS. FASEB J 2005;19:1809–21.
[20] Hofmeijer J, van Putten MJ. Ischemic cerebral damage: an appraisal of synaptic failure. Stroke 2012;43:607–15.
[21] Iadecola C, Anrather J. The immunology of stroke: from mechanisms to translation. Nat Med 2011;17:796–808.
[22] Jenssen H, Aspmo SI. Serum stability of peptides. Methods Mol Biol 2008;494:177–86.
[23] Jiang X, Kim HE, Shu H, Zhao Y, Zhang H, Kofron J, et al. Distinctive roles of PHAP proteins and prothymosin-alpha in a death regulatory pathway. Science 2003;299:223–6.
[24] Karapetian RN, Evstafieva AG, Abaeva IS, Chichkova NV, Filonov GS, Rubtsov YP, et al. Nuclear oncoprotein prothymosin alpha is a partner of Keap1: implications for expression of oxidative stress-protecting genes. Mol Cell Biol 2005;25:1089–99.
[25] Korada S, Zheng W, Basilico C, Schwartz ML, Vaccarino FM. Fibroblast growth factor 2 is necessary for the growth of glutamate projection neurons in the anterior neocortex. J Neurosci 2002;22:863–75.
[26] Krysl D, Deykun K, Lambert L, Pokorny J, Mares J. Perifocal and remote blood–brain barrier disruption in cortical photothrombotic ischemic lesion and its modulation by the choice of anesthesia. J Physiol Pharmacol 2012;63:127–32.
[27] Lal A, Kawai T, Yang X, Mazan-Mamczarz K, Gorospe M. Antiapoptotic function of RNA-binding protein HuR effected through prothymosin alpha. EMBO J 2005;24:1852–62.
[28] Madinier A, Bertrand N, Mossiat C, Prigent-Tessier A, Beley A, Marie C, et al. Microglial involvement in neuroplastic changes following focal brain ischemia in rats. PLoS ONE 2009;4:e8101.
[29] Maiese K, Li F, Chong ZZ. Erythropoietin in the brain: can the promise to protect be fulfilled? Trends Pharmacol Sci 2004;25:577–83.
[30] Mosoian A, Teixeira A, Burns CS, Sander LE, Gusella LG, He C, et al. Prothymosin-α inhibits HIV-1 via Toll-like receptor 4-mediated type I interferon induction. Proc Natl Acad Sci USA 2010;107:10178–83.
[31] Neroev VV, Zueva MV, Kalamkarov GR. Molecular mechanisms of retinal ischemia. Vestn Oftalmol 2010;126:59–64.
[32] Osborne NN, Casson RJ, Wood JP, Chidlow G, Graham M, Melena J. Retinal ischemia: mechanisms of damage and potential therapeutic strategies. Prog Retin Eye Res 2004;23:91–147.
[33] Padmanabhan B, Nakamura Y, Yokoyama S. Structural analysis of the complex of Keap1 with a prothymosin alpha peptide. Acta Crystallogr Sec F Struct Biol Cryst Commun 2008;64:233–8.
[34] Paolucci S, Antonucci G, Grasso MG, Bragoni M, Coiro P, Angelis DD, et al. Functional outcome of ischemic and hemorrhagic stroke patients after inpatient rehabilitation: a matched comparison. Stroke 2003;34:2861–5.
[35] Paul R, Zhang ZG, Eliceiri BP, Jiang Q, Boccia AD, Zhang RL, et al. Src deficiency or blockade of Src activity in mice provides cerebral protection following stroke. Nat Med 2001;7:222–7.
[36] Pierluigi B, D'Angelo C, Fallarino F, Moretti S, Zelante T, Bozza S, et al. Thymosin alpha1: the regulator of regulators? Ann NY Acad Sci 2010;1194:1–5.

[37] Prasad SS, Kojic L, Wen YH, Chen Z, Xiong W, Jia W, et al. Retinal gene expression after central retinal artery ligation: effects of ischemia and reperfusion. Invest Ophthalmol Vis Sci 2010;51:6207–19.
[38] Sato AK, Viswanathan M, Kent RB, Wood CR. Therapeutic peptides: technological advances driving peptides into development. Curr Opin Biotechnol 2006;17:638–42.
[39] Schaar KL, Brenneman MM, Savitz SI. Functional assessments in the rodent stroke model. Exp Transl Stroke Med 2010;2:13.
[40] Sims NR, Muyderman H. Mitochondria, oxidative metabolism and cell death in stroke. Biochim Biophys Acta 2010;1802:80–91.
[41] Siren AL, Fratelli M, Brines M, Goemans C, Casagrande S, Lewczuk P, et al. Erythropoietin prevents neuronal apoptosis after cerebral ischemia and metabolic stress. Proc Natl Acad Sci USA 2001;98:4044–9.
[42] Skopeliti M, Kratzer U, Altenberend F, Panayotou G, Kalbacher H, Stevanovic S, et al. Proteomic exploitation on prothymosin alpha-induced mononuclear cell activation. Proteomics 2007;7:1814–24.
[43] Skopeliti M, Iconomidou VA, Derhovanessian E, Pawelec G, Voelter W, Kalbacher H, et al. Prothymosin alpha immunoactive carboxyl-terminal peptide TKKQKTDEDD stimulates lymphocyte reactions, induces dendritic cell maturation and adopts a beta-sheet conformation in a sequence-specific manner. Mol Immunol 2009;46:784–92.
[44] Ueda H, Fujita R. Cell death mode switch from necrosis to apoptosis in brain. Biol Pharm Bull 2004;27:950–5.
[45] Ueda H, Fujita R, Yoshida A, Matsunaga H, Ueda M. Identification of prothymosin-alpha1, the necrosis-apoptosis switch molecule in cortical neuronal cultures. J Cell Biol 2007;176:853–62.
[46] Ueda H. Prothymosin alpha plays a key role in cell death mode-switch, a new concept for neuroprotective mechanisms in stroke. Naunyn Schmiedebergs Arch Pharmacol 2008;377:315–23.
[47] Ueda H. Prothymosin alpha and cell death mode switch, a novel target for the prevention of cerebral ischemia-induced damage. Pharmacol Ther 2009;123:323–33.
[48] Ueda H, Matsunaga H, Uchida H, Ueda M. Prothymosin alpha as robustness molecule against ischemic stress to brain and retina. Ann NY Acad Sci 2010;1194:20–6.
[49] Ueda H, Matsunaga H, Halder SK. Prothymosin α plays multifunctional cell robustness roles in genomic, epigenetic, and nongenomic mechanisms. Ann NY Acad Sci 2012;1269:34–43.
[50] Ueda H, Matsunaga H, Halder SK. Prothymosin a – a novel endogenous neuroprotective polypeptide against ischemic damages. In: Nyberg FJ, editor. Neuropeptides in neuroprotection and neuroregeneration. CRC Press; 2012. p. 128–43.
[51] Witmer MT, Pavan PR, Fouraker BD, Levy-Clarke GA. Acute retinal necrosis associated optic neuropathy. Acta Ophthalmol 2011;89:599–607.
[52] White BC, Sullivan JM, DeGracia DJ, O'Neil BJ, Neumar RW, Grossman LI, et al. Brain ischemia and reperfusion: molecular mechanisms of neuronal injury. J Neurol Sci 2000;179:1–33.
[53] Yin KJ, Deng Z, Huang H, Hamblin M, Xie C, Zhang J, et al. miR-497 regulates neuronal death in mouse brain after transient focal cerebral ischemia. Neurobiol Dis 2010;38:17–26.

Cell Mol Neurobiol (2012) 32:59–66
DOI 10.1007/s10571-011-9734-x

ORIGINAL RESEARCH

Regional Distribution and Cell Type-Specific Subcellular Localization of Prothymosin Alpha in Brain

Sebok Kumar Halder · Hiroshi Ueda

Received: 31 May 2011 / Accepted: 27 June 2011 / Published online: 13 July 2011

Abstract Prothymosin alpha (ProTα) is an acidic nuclear protein implicated in several cellular functions including cell survival. ProTα is found in the central nervous system, but the regional and cell type-specific expression patterns are not known. In this study, our immunohistochemical analysis demonstrated that ProTα is expressed ubiquitously throughout adult brain with difference in the intensity of region-specific protein reactivity. Interestingly, the highest ProTα signals were observed in the brain regions relevant to neurogenesis, such as sub-ventricular zone, granular cell layer of dentate gyrus, as well as granule cell layer of olfactory bulb. Strong immunoreactivity was also found in habenula, ependymal cells lining the dorsal third and fourth ventricle, and in neurons in the Purkinje cell layer of cerebellum. We showed that ProTα was strictly localized in the nuclei of neurons, while it was found in the cytosolic space of astroglial and microglial processes and cell body in the adult brain. To clarify the phenomenon underlying cytosolic localization of ProTα in non-neuronal cells, ZVAD-fmk, a caspase-3 inhibitor, was delivered intracerebroventricularly in the brain. At the follow-up 24 h after ZVAD-fmk injection, we found that nuclear intensity of ProTα was significantly increased in astrocytes, whereas the ProTα expression was not affected in microglia. The present study would contribute toward better understanding of physiological and pathophysiological roles of ProTα in the brain.

Keywords Subcellular localization · Neurogenesis · Caspase-3 · Habenula · Ependymal cell · Purkinje cell

S. K. Halder · H. Ueda (✉)
Division of Molecular Pharmacology and Neuroscience,
Nagasaki University Graduate School of Biomedical Sciences,
1-14 Bunkyo-machi, Nagasaki 852-8521, Japan
e-mail: ueda@nagasaki-u.ac.jp

Abbreviations

ProTα	Prothymosin alpha
SVZ	Sub-ventricular zone
LV	Lateral ventricle
3V	Third ventricle
4V	Fourth ventricle
CA	Cornu ammonis
Str rad	Stratum radiatum
DG	Dentate gyrus
GCL	Granular cell layer
i.c.v.	Intracerebroventricular
Z-VAD-fmk	Z-Val-Ala-Asp fluoromethyl ketone
DAB	3,3'-diaminobenzidine tetrahydrochloride
Amyg	Amygdala

Introduction

Prothymosin alpha (ProTα) is a small (12.6 kDa), nuclear protein that belongs to alpha-thymosin family, and widely distributed in variety of tissues, such as thymus, spleen, lung, kidney, liver, and brain (Haritos et al. 1984; Pineiro et al. 2000). ProTα, a signal peptide-deficient protein, is associated with cell functions, such as proliferation, division, and survival in various cells (Karapetian et al. 2005; Letsas and Frangou-Lazaridis 2006; Jiang et al. 2003; Gomez-Marquez 2007; Ueda 2008), and with genomic actions such as binding to linker histone H1, DNA packaging (Papamarcaki and Tsolas 1994; Diaz-Jullien et al. 1996; George and Brown 2010), chromatin remodeling (Gomez-Marquez 2007), and regulation of transcription (Martini et al. 2000); Karetsou et al. 2002). In addition to these intracellular functions, there are also several reports

about the immunoregulatory role of extracellular ProTα, such as activation of major histocompatibility complex (MHC) expression (Baxevanis et al. 1992), induction of antitumor and antiviral activity (Garbin et al. 1997; Mosoian et al. 2006), activation of immune cells, and cytokine production (Pineiro et al. 2000; Skopeliti et al. 2007). There is an interesting report that ProTα induces an immunosuppressive activity against viral infection through the activation of Toll-like receptor-4 (Mosoian et al. 2010). Although ProTα has been detected in mammalian tissues, very little is known about cellular and biological roles of ProTα in the nervous system. Recently, ProTα has been identified as a unique cell death regulatory molecule in that it converts the intractable cell death necrosis into the controllable apoptosis, which is in turn inhibited by brain-derived neurotrophic factor/BDNF (Ueda et al. 2007). In addition, the administration of ProTα also inhibited the cerebral and retinal ischemia-induced necrosis as well as apoptosis through up-regulation of BDNF or erythropoietin/EPO (Ueda 2009; Fujita et al. 2009; Ueda et al. 2010). The most recent investigation demonstrate that ProTα is localized in the nuclei of cultured cortical neurons and astrocytes (Matsunaga and Ueda 2010). However, the pattern of ProTα expression in cells in the central nervous system is yet unknown. In this study, we attempted to see the regional distribution and cell type-specific subcellular localization of ProTα in mouse brain.

Materials and Methods

Animals

Male MP-BL mice weighing 20–25 g were used for all the experiments. Mice were kept in a room maintained at constant temperature (21 ± 2°C) and relative humidity (55 ± 5%) with an automatic 12 h light/dark cycle with free access to standard laboratory diet and tap water. All the procedures were formally approved by Nagasaki University Animal Care Committee.

Drug Treatments

Z-Val-Ala-Asp fluoromethyl ketone (Z-VAD-fmk) was purchased from Sigma-Aldrich, St. Louis, USA. Z-VAD-fmk was dissolved in dimethyl sulfoxide (DMSO) and finally diluted in artificial cerebrospinal fluid (ACSF). Z-VAD-fmk was delivered intracerebroventricularly (i.c.v.) at a dose of 1 μg/5 μl in the mouse brain using Hamilton syringe. Control mice were treated with equal volume of ACSF in a same manner. Mice were sacrificed at 3 and 24 h after injection.

Tissue Preparations

Mice were deeply anesthetized with sodium pentobarbital (50 mg/kg) and perfused transcardially with 0.1 M potassium-free phosphate buffered saline (K^+-free PBS, pH 7.4) followed by 4% paraformaldehyde (PFA) in 0.1 M K^+-free PBS. Brain was then quickly removed and post-fixed in 4% PFA for 3 h, and immediately transferred to 25% sucrose solution (in 0.1 M K^+-free PBS) overnight for cryoprotection. Brain was frozen in cryoembedding compound, and the coronal brain sections were prepared at 30-μm thickness by cryostat for immunohistochemical analysis.

Characterization of Anti-ProTα Antibody

Anti-ProTα antibody (mouse monoclonal IgG 2F11; Enzo Life Sciences Int., PA, USA) recognizes *N*-terminal region of ProTα spanning amino acids 1–31. Immunohistochemical analysis was used for the characterization of anti-ProTα antibody against ProTα in mouse brain. The isolation and purification of recombinant ProTα used in this experiment were performed following the protocol as described previously (Fujita et al. 2009). To confirm that the immunoreactivity of ProTα is specific, another set of experiments using anti-ProTα IgG primary antibody pre-absorbed with purified mouse recombinant ProTα (rProTα) for 30 min (10:1 rProTα:anti-ProTα IgG [w/w]; antibody dilution 1:1,000 in 1% blocking buffer) was performed. Then, fluorescent immunostaining was performed by incubating brain coronal sections with preabsorbed anti-ProTα antibody. For control, brain sections were incubated with anti-ProTα IgG primary antibody (1:1,000; Enzo Life Sciences Int., PA, USA).

Immunohistochemical Analysis

To perform 3,3′-diaminobenzidine tetrahydrochloride (DAB) immunostaining, the floating coronal brain sections were incubated with 1% H_2O_2 solution for 30 min and washed with 0.1% Triton X-100 in phosphate-buffered saline (PBST). The sections were incubated with blocking buffer containing 2% BSA in PBST and goat antiserum to mouse IgG (1:50; Cappel laboratories, PA, USA). Sections were then incubated with anti-ProTα IgG primary antibodies (1:1,000; mouse monoclonal IgG 2F11; Enzo Life Sciences Int., PA, USA) in 1% blocking buffer overnight at 4°C. Then, the sections were incubated with biotin-conjugated secondary antibody (1:500; goat polyclonal anti-mouse IgG, Invitrogen, CA, USA) and subsequently treated with avidin–biotin peroxidase solution (ABC kit, Vectastain Vector, USA). ProTα reactivity was visualized by incubation with a solution containing 0.02% DAB (Dojindo,

Kumamoto, Japan), 0.005% H_2O_2 (WAKO, Japan) in 0.05 M Tris–HCl buffer (pH 7.6), 1% cobalt chloride ($CoCl_2$), and nickel sulfate 1% $NiSO_4$ solution (Sigma-Aldrich, St. Louis, USA). Coronal brain sections were dehydrated through a series of ethanol solutions, xylene, and cover-slipped with Permount (Fisher Scientific, Waltham, MA, USA). Immunoreactivity of ProTα-positive cells (black reaction products) was analyzed using BZ Image Measurement Software (Keyence, Tokyo, Japan). For fluorescence immunostaining, coronal brain sections were washed with K^+-free PBS and incubated with 50% methanol followed by 100% methanol for 10 min. Samples were pretreated with blocking buffer containing 2% BSA in 0.1% PBST and incubated overnight at 4°C with following primary antibodies: anti-MAP2 (1:500, rabbit polyclonal antibody, Chemicon, CA, USA); anti-GFAP (1:500, rabbit polyclonal antibody, Dako, Denmark); and anti-Iba1 (1:1,000, rabbit polyclonal antibody, WAKO, Japan); anti-ProTα IgG (1:1,000; mouse monoclonal IgG 2F11; Enzo Life Sciences Int., PA, USA). Brain sections were then incubated with FITC-conjugated Alexa Fluor 594-conjugated anti-rabbit IgG and Alexa Fluor 488-conjugated anti-mouse IgG secondary antibodies (1:300; Molecular Probes, CA, USA). The nuclei were visualized through Hoechst 33342 (1:10,000, Molecular Probes, CA, USA). Samples were then washed thoroughly with PBS, cover-slipped with Perma Fluor (Thermo Shandon, Pittsburgh, PA, USA), and examined under a confocal microscope imaging system (Axiovert 200 M, Scan module: LSM 5 PASCAL; Carl Zeiss MicroImaging, Inc.) with image browser software (Carl Zeiss MicroImaging, Inc.), and also with BZ Image Measurement Software (Keyence, Tokyo, Japan). For image preparation, immunohistochemical images were adjusted when necessary for contrast and brightness using Adobe Photoshop (San Jose, CA, USA).

Results

Regional Distribution of ProTα in Brain

The diaminobenzidine (DAB) immunohistochemical analysis using mouse brain coronal sections show that ProTα is expressed ubiquitously throughout the mouse brain (Fig. 1a–d). The strength of ProTα immunoreactivity was different in the several regions of hippocampus (Fig. 1e). Highly magnifying observation of hippocampal section revealed that the signals in the pyramidal neuronal cell layer of cornu ammonis (CA1-3) were stronger than in cells in the stratum radiatum and stratum oriens (Fig. 1f). Among the regions of hippocampus, the highest ProTα signals were observed in neurons of granular cell layer in dentate gyrus, the popular zone of neurogenesis (Fig. 1g).

Similar strong immunoreactivity was found in the subventricular zone (SVZ), few cells in the striatum close to SVZ (Fig. 1h), and in some cells in the granule cell layer (GC) of olfactory bulb (Fig. 1i). Stronger signals were also observed in the ependymal cell layer lining the lateral ventricle, a part of SVZ (Fig. 1h), and in the ependymal cell lining the fourth ventricle of cerebellum (Fig. 1j), whereas relatively weaker signals in peri-ventricular nucleus were observed in the hypothalamus (Fig. 1k).

In addition, we found strong signals in the choroids plexus (CP), ependymal cell layer lining the dorsal third ventricle (3DV), and habenula (Fig. 1l, m). Most interestingly, the strongest signals were observed in neurons in Purkinje cell layer in cerebellum (Fig. 1n).

Cell type-Specific Subcellular Localization of ProTα

To examine the cell type-specific expression of ProTα in mouse brain, fluorescent immunostaining of brain coronal sections was performed with antibodies against ProTα and specific cell markers, such as MAP2 for neurons, GFAP for astrocytes, and Iba-1 for microglia. Our triple immunostaining data revealed that ProTα was expressed and strictly localized in the nuclei of MAP2-positive neurons in CA1 pyramidal neuronal cell layer of hippocampus (Fig. 2a). On the other hand, ProTα immunoreactivity was also observed in both GFAP-positive astrocytes and Iba-1-positive microglia in the stratum radiatum of hippocampus (Fig. 2b, c, respectively). Interestingly, we found that ProTα signal was localized in both cytosolic space of astroglial and microglial processes and cell body in the adult brain. Similar expressions and subcellular localizations were observed in neurons (Fig. 3a, b), astrocytes (Fig. 3c, d) and microglia (Fig. 3e, f) in the striatum, and cortex of brain.

In order to make sure that the signal was specific for ProTα, antibody (mouse monoclonal anti-ProTα IgG, 2F11, Enzo Life Sciences Int., PA, USA) was pretreated with recombinant ProTα for 30 min, and subsequent immunostaining of brain coronal sections was performed. This antibody has been reported to bind to the N-terminal region of ProTα spanning amino acids 1–31. Our findings showed that the addition of recombinant ProTα in antibody completely abolished the ProTα signal in MAP-2-positive neurons (Fig. 2d), GFAP-positive astrocytes (Fig. 2e), and Iba-1-positive microglia (Fig. 2f).

Caspase-3 Inhibitor Redistributes ProTα in Astrocytes

Our previous study reported that caspase-3 activation cleaved off the nuclear localization signal of ProTα in astrocytes and released it from the nucleus (Matsunaga and Ueda 2010). In addition, as adult astrocytes are known to

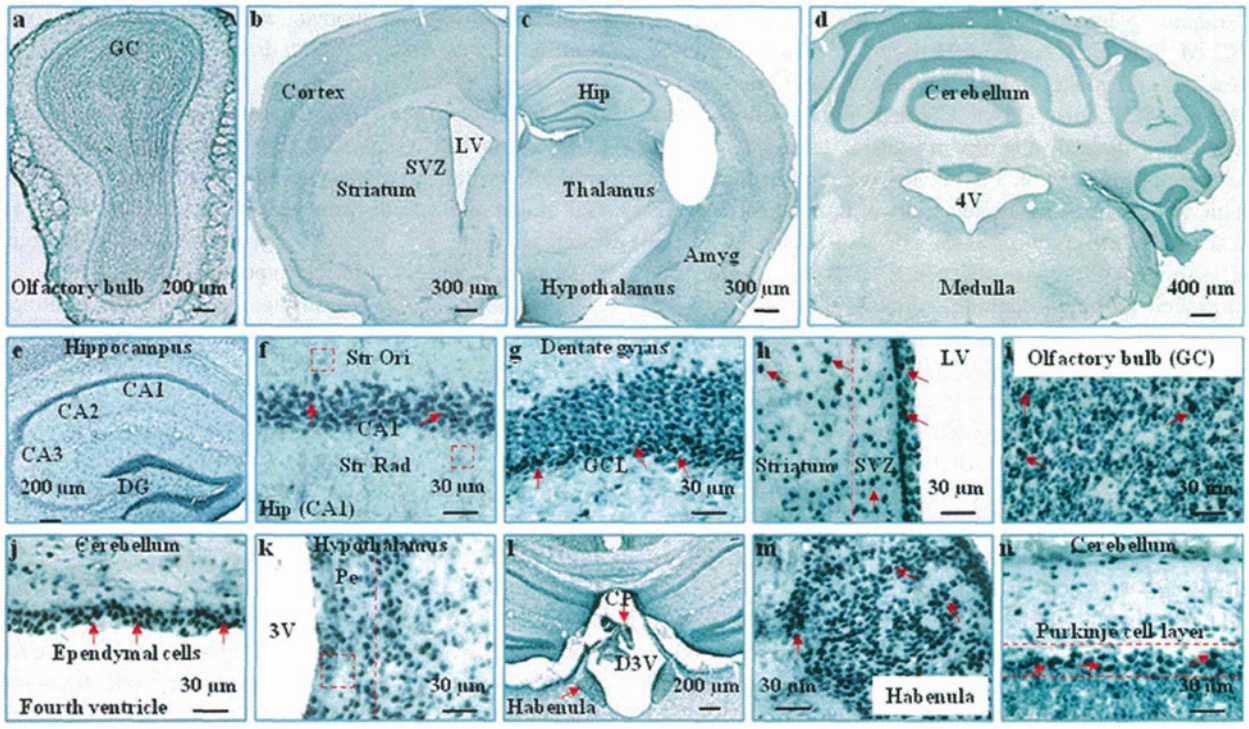

Fig. 1 Regional distribution of ProTα in the adult mouse brain. **a–n** DAB immunohistochemical analysis of coronal brain sections was performed, and ProTα immunoreactivity was observed using antibody against ProTα in brain. **a–d** Low magnification views of coronal sections show the general immunoreactivity of ProTα in the brain. DAB immunostaining data show the ProTα signals in the various regions of hippocampus (**e**) including cornu ammonis (CA1-3), stratum radiatum and stratum oriens (**f**) and dentate gyrus (**g**). ProTα signals are also found in sub-ventricular zone (SVZ) of the lateral ventricle (LV) and in some cells in the striatum close to the SVZ (**h**), granule cell layer (GC) of olfactory bulb (**i**), ependymal cell layer lining the fourth ventricle (**j**), periventricular nucleus (Pe) in hypothalamus (**k**), choroids plexus (CP) and ependymal cells lining dorsal third ventricle (**l**), habenula (**l**, **m**), and in purkinje cell layer in cerebellum (**n**). In figures **f–n**, the *arrowhead* points indicate the higher intensity of ProTα reactivity in brain. *Scale bars* **a**, **e**, **l** 200 μm, **b**, **c** 300 μm, **d** 400 μm, **f–k**, **m**, **n** 30 μm

have caspase-3 activity in the nucleus (Duran-Vilaregut et al. 2010); we attempted to see whether this protease inhibitor might redistribute ProTα. When Z-VAD-fmk, a caspase-3 inhibitor, was administered (i.c.v.) in brain and triple immunostaining performed at 3 and 24 h after injection, nuclear ProTα intensity was significantly increased in the nucleus of astrocytes in the stratum radiatum of hippocampus at 3 h (data are not shown) to 24 h (Fig. 4b), as compared to the control (Fig. 4a). On the other hand, no change in ProTα localization was observed in microglia at the same period after injection (Fig. 4c, d).

Discussion

In this study, we demonstrated that ProTα is expressed ubiquitously, but its regional expression varied throughout the adult mouse brain. Higher expression was found in dentate gyrus of hippocampus, SVZ of lateral ventricle and olfactory bulb, the regions which have been described as the popular areas for neurogenesis (Hack et al. 2005; Gould 2007; Zhao et al. 2008; Jin et al. 2010). ProTα expression was relatively higher in the granular cell layer (GCL) of dentate gyrus than the molecular layer. In the SVZ, more intense expression was found in the ependymal cell layer. It should be noted that some cells in the striatum close to the SVZ and in the granule cell layer of olfactory bulb also express intense signals. Taking it into consideration that GCL is the major locus for adult neurogenesis and newly born neurons in the adult SVZ migrate tangentially along the rostral migratory stream (RMS) to olfactory bulb (Brill et al. 2009) and also in the striatum (Ninomiya et al. 2006), it may be speculated that ProTα expression is related to the neurogenesis. However, ProTα expression is also high in the ependymal cells lining the fourth ventricle, where cerebrospinal fluid is produced, but little is known of the relationship of this region to neurogenesis. It is unlikely that the signals in ependymal cells at the edge of ventricle are caused by non-specific staining, since no prominent signals are found in the similar region at the third ventricle.

Higher expression was also observed in choroid plexus, habenula, and Purkinje cell layers of cerebellum. Choroid

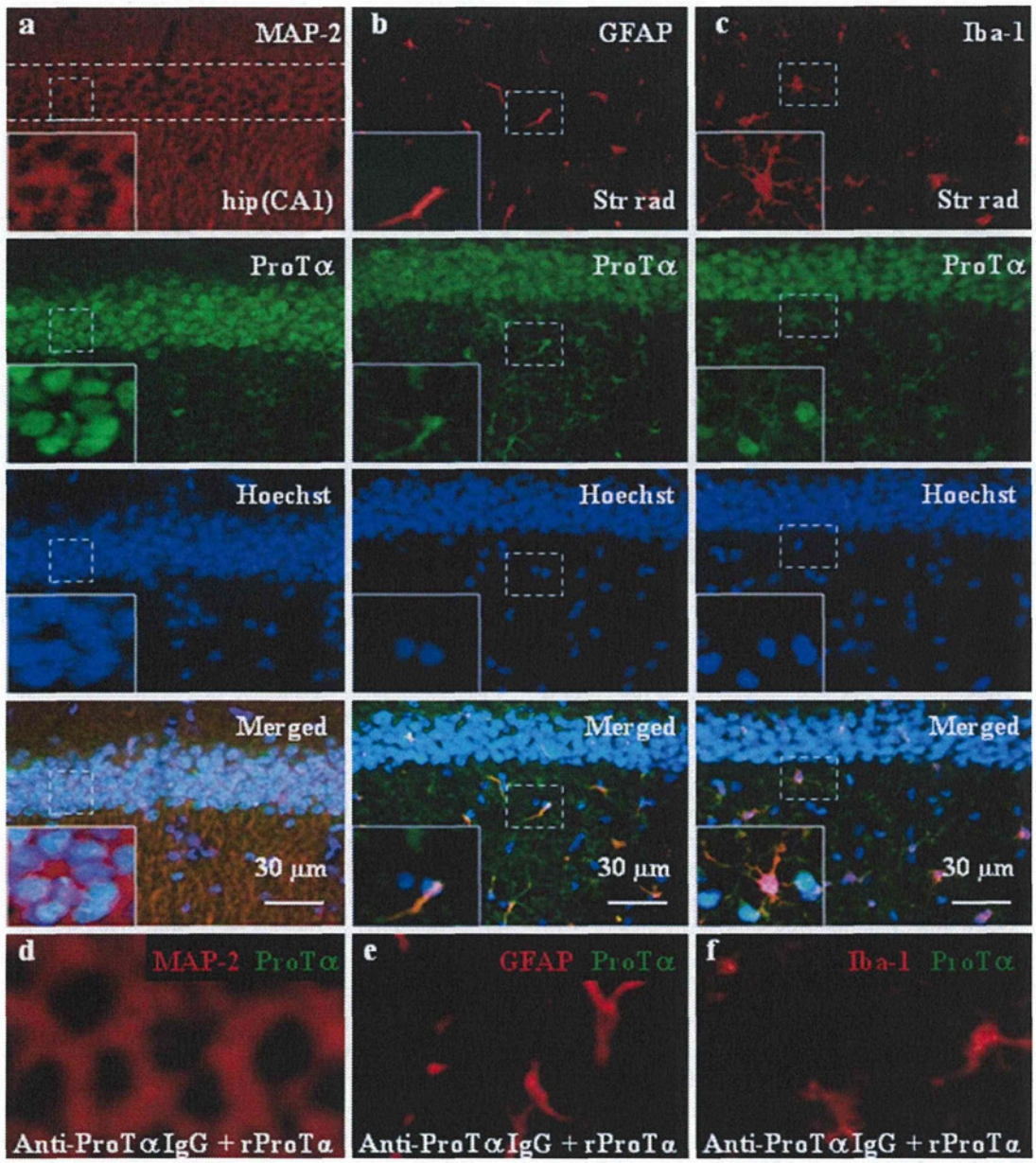

Fig. 2 Cell type-specific sub-cellular localization of ProTα. **a–c** Triple immunofluorescence staining was performed using brain coronal sections. Immunostaining data indicate that ProTα is localized in nucleus in the CA1 pyramidal cell layer neurons indicated by dot lines in the hippocampus (**a** MAP-2, *red*; ProTα, *green*; Hoechst, *blue*). ProTα is localized both in cytosolic space of processes and cell body in astrocytes (**b** GFAP, *red*; ProTα, *green*; Hoechst, *blue*) and microglia (**c** Iba-1, *red*; ProTα, *green*; Hoechst, *blue*) in the stratum radiatum of hippocampus. *Insets* in **a–c** indicate the high-magnification view of ProTα localization noted by *squares*. For antibody characterization, anti-ProTα IgG was pretreated with recombinant ProTα (rProTα) for 30 min, and subsequent double immunostaining of brain coronal sections was performed. Addition of recombinant ProTα in the antibody completely abolished the ProTα signal in MAP-2-positive neurons (**d**), GFAP-positive astrocytes (**e**), and Iba-1-positive microglia (**f**). *Scale bars* **a–c** 30 μm

plexus is mainly involved in the production of cerebrospinal fluid (CSF) and in a variety of neurological disorders (Wolburg and Paulus 2009; Wrede et al. 2009). Recently, habenula has attracted a great deal of attention for its prominent role in the regulation of dopamine and serotonin systems in terms of depression, anxiety, sleep mode, and extrapyramidal motor functions (Lecourtier et al. 2006; Hikosaka 2010). As depression is associated with cell death (Arantes-Goncalves and Coelho 2006; McKernan et al. 2009) and ProTα is a potent neuroprotective protein (Ueda et al. 2007), the role of ProTα in the habenula may be an intriguing subject in the phenotypic analysis of

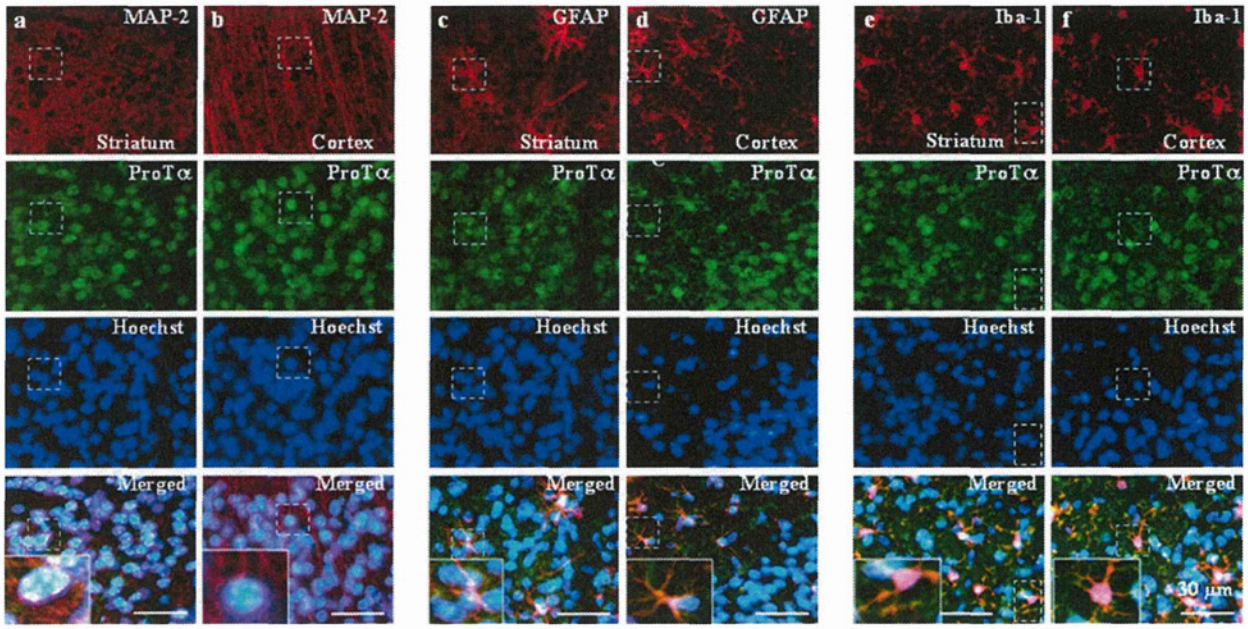

Fig. 3 Cell type-specific sub-cellular localization of ProTα in the striatum and cortex. Triple fluorescence staining of brain coronal indicates that ProTα was localized in nucleus in striatal (**a** MAP-2, *red*; ProTα, *green*; Hoechst, *blue*) and cortical neurons (**b**). ProTα is localized both in cytosolic space of processes and cell body in astrocytes in the striatum (**c** GFAP, *red*; ProTα, *green*; Hoechst, *blue*) and cortex (**d**). The expression of ProTα in the striatal (**e** Iba-1, *red*; ProTα, *green*; Hoechst, *blue*) and cortical microglia (**f**). *Insets* in **a**–**f** indicate the high-magnification view of ProTα localization noted by squares. *Scale bars* 30 μm

ProTα-related transgenic mice. Most interestingly, stronger ProTα signals that were found in neurons in Purkinje cell layer of cerebellum play an important role in movement, posture, and cognitive functions (Jorntell and Hansel 2006; Iscru et al. 2009). In this study we successfully demonstrated the cell type-specific sub-cellular localization of ProTα in adult brain. Detailed immunohistochemical findings revealed that ProTα was strictly confined in the nuclei of neuronal cells, whereas the expression was observed in the cytosolic space of astroglial and microglial processes and cell body in the adult brain. Several investigations demonstrated that ProTα binds to partner histone H1 in the nuclei and helps in DNA packaging (Papamarcaki and Tsolas 1994; Diaz-Jullien et al. 1996; George and Brown 2010), participates in chromatin remodeling (Gomez-Marquez and Rodriguez 1998), and regulates gene transcription (Trumbore and Berger 2000; karetsou et al. 2002). It is evident that ProTα regulates transcriptional activity of the estrogen receptor by sequestering repressor from the estrogen receptor complex (Martini et al. 2000). Therefore, it is suggested that nuclear ProTα may play roles in epigenetic regulation in neurons. In addition to such nuclear functions, ProTα has various putative functions in the cytosol space (Jiang et al. 2003; Karapetian et al. 2005). There is a challenging investigation about ProTα-mediated inhibition of translation by regulating the phosphorylation of eukaryotic elongation factor 2 during mitotic cell division (Vega et al. 1998; Enkemann et al. 1999). ProTα protects cells from oxidative stress through the dissociation of the intranuclear Nrf2–Keap1 complex and facilitates expression of oxidative stress-protecting genes (Karapetian et al. 2005). It has also been hypothesized that ProTα prevents cells from apoptosis through the inhibition of apoptosome formation (Jiang et al. 2003; Letsas and Frangou-Lazaridis 2006). The cytosol expression of ProTα in glial cells may be related to the fact that glial cells have more resistance to cell death stress than neurons.

Recent in vitro study has postulated that ProTα is localized in the nuclei of primary culture of rat embryonic astrocytes (Matsunaga and Ueda 2010). This finding revealed a discrepancy from the present study, in which ProTα is found in both cytosol and nucleus of astrocytes. There are several reports hypothesizing that the fragmentation of ProTα was mediated by caspase-3 enzyme at C-terminal side located within the spacer region bipartite nuclear localization signal (NLS) in ProTα (Rubtsov et al. 1997; Enkemann et al. 2000; Matsunaga and Ueda 2010). It has recently been described that active caspase-3 is present in the nuclei of astrocytes in normal brain (Duran-Vilaregut et al. 2010). Based on these findings, we attempted to see effects of ZVAD-fmk, a caspase-3 inhibitor, and found that nuclear localization of ProTα was significantly increased at 3–24 h in astrocytes after i.c.v administration. Therefore, it is supposed that the C-terminal part possessing NLS of

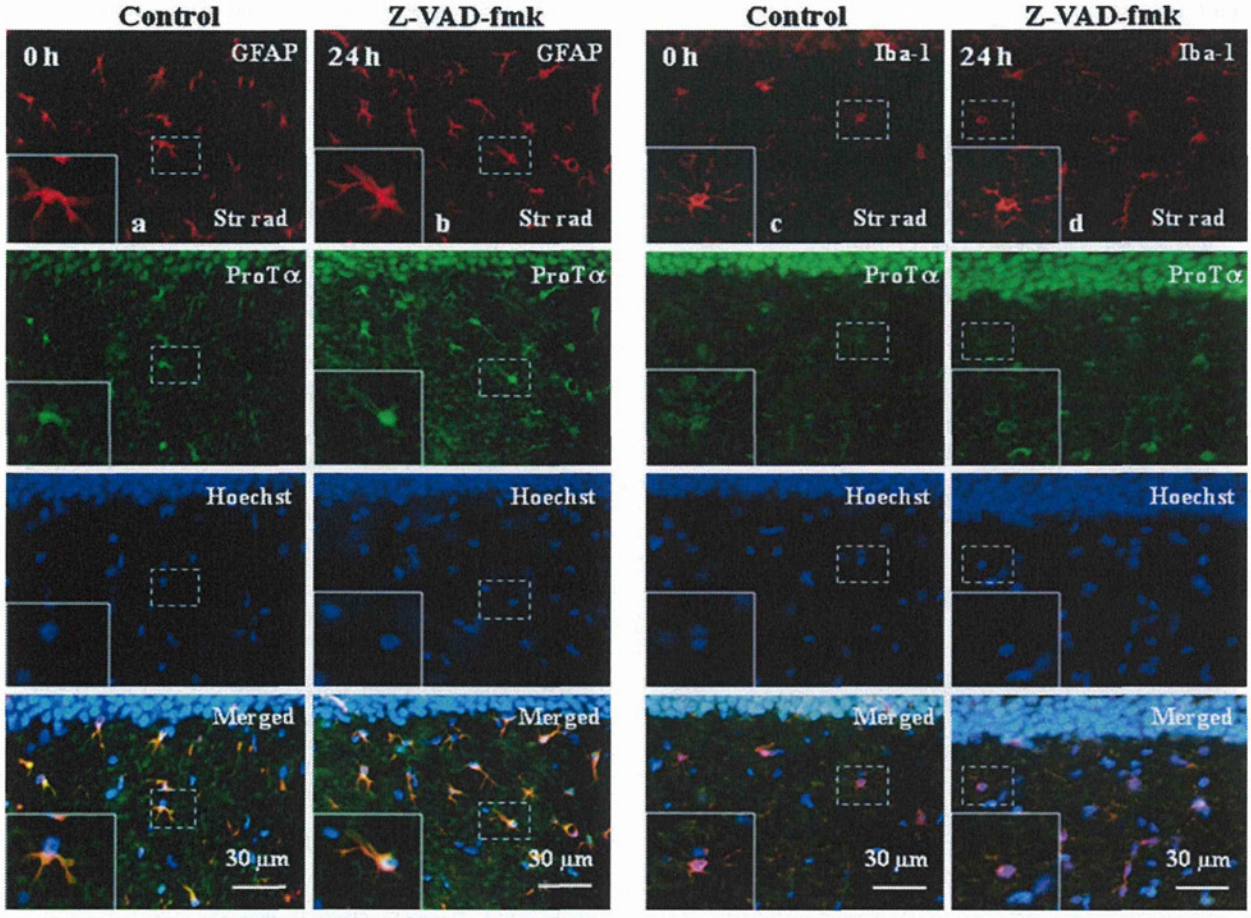

Fig. 4 Redistribution of ProTα by caspase-3 inhibitor treatment in astrocytes. ZVAD-fmk, a caspase-3 inhibitor, was injected intracerebroventricularly (i.c.v.) in mice brain, and ProTα immunostaining was performed at 24 h after treatment. Nuclear intensity of ProTα was significantly increased in astrocytes (**b** GFAP, *red*; ProTα, *green*; Hoechst, *blue*) in the stratum radiatum of hippocampus at 24 h after injection compared to the control (**a**), but there was no change in ProTα signals in microglia (**d** Iba-1, *red*; ProTα, *green*; Hoechst *blue*), compared to the control (**c**). *Insets* in **a–d** indicate the high-magnification view of ProTα localization denoted by *squares*. *Scale bars* 30 μm

ProTα may be cleaved by active caspase-3 in adult astrocytes of normal brain. Similarly, ProTα expression was also observed in both cytosol and nucleus in microglia. However, the expression pattern of ProTα in microglia was unchanged in the ZVAD-fmk-treated brain, though detailed mechanisms underlying this discrepancy in subcellular localization among neurons, astrocytes, and microglia would become the subject of future research. Taken together, the present findings encourage us to investigate the possible intracellular roles of cytosolic ProTα in astrocytes and microglia.

In conclusion, our study demonstrates that ProTα is expressed ubiquitously throughout the adult brain. There are very strong signals observed in some regions, especially in the neurogenesis-related zones in brain. The pattern of ProTα localization in neurons was completely different from that in astrocytes or microglia in the adult brain. Our demonstration would contribute to further understanding of the physiological and pathophysiological roles of ProTα in the brain.

Acknowledgments The authors thank J. Sugimoto for his technical assistance. We also thank H. Matsunaga for his helpful suggestions. The authors thank H. Kurosu for supplying mouse recombinant ProTα. This study was partially supported by Grants-in-Aid for Scientific Research (to H.U., B: 13470490 and 15390028), on Priority Areas—Research on Pathomechanisms of Brain Disorders (to H.U., 17025031, 18023028 and 20023022) from the Ministry of Education, Culture, Sports, Science and Technology (MEXT) and the Health and Labour Sciences Research Grants on Research on Biological Resources and Animal Models for Drug Development (to H.U., H20—Research on Biological Resources and Animal Models for Drug Development-003) from the Ministry of Health, Labour, and Welfare.

References

Arantes-Goncalves F, Coelho R (2006) Depression and treatment. Apoptosis, neuroplasticity and antidepressants. Acta Med Port 19(1):9–20

Baxevanis CN et al (1992) Prothymosin alpha enhances human and murine MHC class II surface antigen expression and messenger RNA accumulation. J Immunol 148(7):1979–1984

Brill MS et al (2009) Adult generation of glutamatergic olfactory bulb interneurons. Nat Neurosci 12(12):1524–1533

Diaz-Jullien C et al (1996) Prothymosin alpha binds histones in vitro and shows activity in nucleosome assembly assay. Biochim Biophys Acta 1296(2):219–227

Duran-Vilaregut J et al (2010) Systemic administration of 3-nitropropionic acid points out a different role for active caspase-3 in neurons and astrocytes. Neurochem Int 56(3):443–450

Enkemann SA et al (1999) Does prothymosin alpha affect the phosphorylation of elongation factor 2? J Biol Chem 274(26): 18644–18650

Enkemann SA et al (2000) Mobility within the nucleus and neighboring cytosol is a key feature of prothymosin-alpha. J Histochem Cytochem 48(10):1341–1355

Fujita RH et al (2009) Prothymosin-alpha plays a defensive role in retinal ischemia through necrosis and apoptosis inhibition. Cell Death Differ 16(2):349–358

Garbin F et al (1997) Prothymosin alpha 1 effects, in vitro, on the antitumor activity and cytokine production of blood monocytes from colorectal tumor patients. Int J Immunopharmacol 19(6): 323–332

George EM, Brown DT (2010) Prothymosin alpha is a component of a linker histone chaperone. FEBS Lett 584(13):2833–2836

Gomez-Marquez J (2007) Function of prothymosin alpha in chromatin decondensation and expression of thymosin beta-4 linked to angiogenesis and synaptic plasticity. Ann N Y Acad Sci 1112:201–209

Gomez-Marquez J, Rodriguez P (1998) Prothymosin alpha is a chromatin-remodelling protein in mammalian cells. Biochem J 333(Pt 1):1–3

Gould E (2007) How widespread is adult neurogenesis in mammals? Nat Rev Neurosci 8(6):481–488

Hack MA et al (2005) Neuronal fate determinants of adult olfactory bulb neurogenesis. Nat Neurosci 8(7):865–872

Haritos AA et al (1984) Distribution of prothymosin alpha in rat tissues. Proc Natl Acad Sci USA 81(5):1391–1393

Hikosaka O (2010) The habenula: from stress evasion to value-based decision-making. Nat Rev Neurosci 11(7):503–513

Iscru E et al (2009) Sensorimotor enhancement in mouse mutants lacking the Purkinje cell-specific Gi/o modulator, Pcp2(L7). Mol Cell Neurosci 40(1):62–75

Jiang X et al (2003) Distinctive roles of PHAP proteins and prothymosin-alpha in a death regulatory pathway. Science 299(5604):223–226

Jin K et al (2010) Transgenic ablation of doublecortin-expressing cells suppresses adult neurogenesis and worsens stroke outcome in mice. Proc Natl Acad Sci USA 107(17):7993–7998

Jorntell H, Hansel C (2006) Synaptic memories upside down: bidirectional plasticity at cerebellar parallel fiber-Purkinje cell synapses. Neuron 52(2):227–238

Karapetian RN et al (2005) Nuclear oncoprotein prothymosin alpha is a partner of Keap1: implications for expression of oxidative stress-protecting genes. Mol Cell Biol 25(3):1089–1099

Karetsou Z et al (2002) Prothymosin alpha interacts with the CREB-binding protein and potentiates transcription. EMBO Rep 3(4):361–366

Lecourtier L et al (2006) Habenula lesions alter synaptic plasticity within the fimbria-accumbens pathway in the rat. Neuroscience 141(2):1025–1032

Letsas KP, Frangou-Lazaridis M (2006) Surfing on prothymosin alpha proliferation and anti-apoptotic properties. Neoplasma 53(2): 92–96

Martini PG et al (2000) Prothymosin alpha selectively enhances estrogen receptor transcriptional activity by interacting with a repressor of estrogen receptor activity. Mol Cell Biol 20(17): 6224–6232

Matsunaga H, Ueda H (2010) Stress-induced non-vesicular release of prothymosin-alpha initiated by an interaction with S100A13, and its blockade by caspase-3 cleavage. Cell Death Differ 17(11): 1760–1772

McKernan DP et al (2009) "Killing the blues": a role for cellular suicide (apoptosis) in depression and the antidepressant response? Prog Neurobiol 88(4):246–263

Mosoian A et al (2006) Novel function of prothymosin alpha as a potent inhibitor of human immunodeficiency virus type 1 gene expression in primary macrophages. J Virol 80(18):9200–9206

Mosoian A et al (2010) Prothymosin-alpha inhibits HIV-1 via toll-like receptor 4-mediated type I interferon induction. Proc Natl Acad Sci USA 107(22):10178–10183

Ninomiya M et al (2006) Enhanced neurogenesis in the ischemic striatum following EGF-induced expansion of transit-amplifying cells in the subventricular zone. Neurosci Lett 403(1–2):63–67

Papamarcaki T, Tsolas O (1994) Prothymosin alpha binds to histone H1 in vitro. FEBS Lett 345(1):71–75

Pineiro A et al (2000) Fifteen years of prothymosin alpha: contradictory past and new horizons. Peptides 21(9):1433–1446

Rubtsov YP et al (1997) Mutational analysis of human prothymosin alpha reveals a bipartite nuclear localization signal. FEBS Lett 413(1):135–141

Skopeliti M et al (2007) Proteomic exploitation on prothymosin alpha-induced mononuclear cell activation. Proteomics 7(11): 1814–1824

Trumbore MW, Berger SL (2000) Prothymosin alpha is a nonspecific facilitator of nuclear processes: studies of run-on transcription. Protein Expr Purif 20(3):414–420

Ueda H (2008) Prothymosin alpha plays a key role in cell death mode-switch, a new concept for neuroprotective mechanisms in stroke. Naunyn Schmiedebergs Arch Pharmacol 377(4–6):315–323

Ueda H (2009) Prothymosin alpha and cell death mode switch, a novel target for the prevention of cerebral ischemia-induced damage. Pharmacol Ther 123(3):323–333

Ueda H et al (2007) Identification of prothymosin-alpha1, the necrosis-apoptosis switch molecule in cortical neuronal cultures. J Cell Biol 176(6):853–862

Ueda H et al (2010) Prothymosin alpha as robustness molecule against ischemic stress to brain and retina. Ann N Y Acad Sci 1194:20–26

Vega FV et al (1998) Prothymosin alpha stimulates $Ca2^{+}$-dependent phosphorylation of elongation factor 2 in cellular extracts. J Biol Chem 273(17):10147–10152

Wolburg H, Paulus W (2009) Choroid plexus: biology and pathology. Acta Neuropathol 119(1):75–88

Wrede B et al (2009) Atypical choroid plexus papilloma: clinical experience in the CPT-SIOP-2000 study. J Neurooncol 95(3): 383–392

Zhao C et al (2008) Mechanisms and functional implications of adult neurogenesis. Cell 132(4):645–660

Journal of Neurochemistry

JOURNAL OF NEUROCHEMISTRY | 2012 | 123 | 262–275

doi: 10.1111/j.1471-4159.2012.07897.x

ORIGINAL ARTICLE

Neuron-specific non-classical release of prothymosin alpha: a novel neuroprotective damage-associated molecular patterns

Sebok Kumar Halder, Hayato Matsunaga and Hiroshi Ueda

Department of Molecular Pharmacology and Neuroscience, Nagasaki University Graduate School of Biomedical Sciences, Nagasaki, Japan

Abstract

Prothymosin alpha (ProTα), a nuclear protein devoid of signal sequence, has been shown to possess a number of cellular functions including cell survival. Most recently, we demonstrated that ProTα is localized in the nuclei of neurons, while it is found in both nuclei and cytoplasm in the astrocytes and microglia of adult brain. However, the cell type-specific non-classical release of ProTα under cerebral ischemia is yet unknown. In this study, we report that ProTα is non-classically released along with S100A13 from neurons in the hippocampus, striatum and somatosensory cortex at 3 h after cerebral ischemia, but amlexanox (an anti-allergic compound) reversibly blocks this neuronal ProTα release. We found that none of ProTα is released from astrocytes and microglia under ischemic stress. Indeed, ProTα intensity is increased gradually in astrocytes and microglia through 24 h after the cerebral ischemia. Interestingly, Z-Val-Ala-Asp fluoromethyl ketone, a caspase 3 inhibitor, pre-treatment induces ProTα release from astrocytes in the ischemic brain, but this release is reversibly blocked by amlexanox. However, Z-Val-Ala-Asp fluoromethyl ketone as well as amlexanox has no effect on ProTα distribution in microglia upon cerebral ischemia. Taken together, these results suggest that only neurons have machineries to release ProTα upon cerebral ischemic stress *in vivo*.

Keywords: apoptosis, cerebral ischemia, necrosis, neuroprotective DAMPs, non-classical release, S100A13.

J. Neurochem. (2012) **123**, 262–275.

The ischemia in the central nervous system is a complex pathophysiological condition, in which neuronal necrosis in the ischemic core causes progressive secretion of cytotoxic mediators, which in turns further cause extended neuronal death (Danton and Dietrich 2003; Swanson *et al.* 2004; Ueda 2009; Niizuma *et al.* 2010; Zhao and Rampe 2010). A wide variety of intracellular molecules termed as damage-associated molecular patterns (DAMPs) are secreted into the extracellular environment upon necrotic/ischemic stress and play key roles in such deterioration of cellular damages (Rubartelli and Lotze 2007; Kono and Rock 2008; Chen and Nunez 2010; Schmidt and Tuder 2010; Zitvogel *et al.* 2010; Pisetsky 2011). Among these molecules, high mobility group box-1 (HMGB-1) is a representative DAMPs protein, which is extracellularly released from the nuclei of neurons upon ischemic damages (Lotze and Tracey 2005; Liu *et al.* 2007; Muhammad *et al.* 2008; Qiu *et al.* 2008; Sims *et al.* 2010; Yang *et al.* 2010; Zhang *et al.* 2011). However, there is also a case that neuroprotective molecule, such as prothymosin alpha (ProTα), is released into the extracellular milieu upon ischemic/necrotic stress in culture experiments (Ueda and Fujita 2004; Fujita and Ueda 2007; Ueda *et al.* 2007, 2010; Fujita *et al.* 2009; Ueda 2009). In this sense, ProTα may be called as a new member of cytoprotective DAMPs molecules.

ProTα is a nuclear protein and functionally implicated with cellular proliferation and survival (Pineiro *et al.* 2000; Jiang

Received May 15, 2012; revised manuscript received July 24, 2012; accepted July 25, 2012.

Address correspondence and reprint requests to Dr Hiroshi Ueda, Department of Molecular Pharmacology and Neuroscience, Nagasaki University Graduate School of Biomedical Sciences, 1-14 Bunkyo-machi, Nagasaki 852-8521, Japan. E-mail: ueda@nagasaki-u.ac.jp

Abbreviations used: Amx, amlexanox; CA, cornu ammonis; DAMPs, damage-associated molecular patterns; HMGB-1, high mobility group box-1; Hip, hippocampus; i.c.v., intracerebroventricular; GFAP glial fibrillary acidic protein, intracerebroventricular; MAP-2, Microtubule-associated protein; PBS, phosphate-buffered saline; ProTα, prothymosin alpha; Str rad, stratum radiatum; tMCAO, transient middle cerebral artery occlusion; Z-VAD-fmk, Z-Val-Ala-Asp fluoromethyl ketone.

et al. 2003; Gomez-Marquez 2007; Ueda 2009), chromatin remodeling (Gomez-Marquez and Rodriguez 1998), DNA packaging (Diaz-Jullien *et al.* 1996; George and Brown 2010), and regulation of transcription (Martini *et al.* 2000; Karetsou *et al.* 2002). In addition to this, extracellular roles of ProTα have also been reported (Baxevanis *et al.* 1992; Garbin *et al.* 1997; Mosoian *et al.* 2006). There is an exciting report about the involvement of Toll-like receptor-4 in ProTα-induced immunoprotection against virus (Mosoian *et al.* 2010). The recent *in vitro* investigations described that ProTα is localized in nuclei of both cultured cortical neurons and embryonic astrocytes, and that is extracellularly released from these cells upon ischemic stress (Matsunaga and Ueda 2010). The mode of ischemia-induced non-classical release of ProTα was characterized in the experiments using C6 astroglioma cells *in vitro* (Matsunaga and Ueda 2010). This study explained that ProTα is first diffused from the nucleus to cytosol, and in turn immediately co-released to the extracellular space with S100A13 (a Ca^{2+}-binding cargo protein) and this release is reversibly blocked by amlexanox, an anti-allergic drug.

Most recently, we demonstrated that ProTα is strictly localized in the nucleus of adult brain neurons, whereas it is expressed both in the cell body and cytosolic space of processes in the astrocytes and microglia, an indication of big difference between *in vitro* and *in vivo* studies in terms of ProTα localization in astrocytes (Matsunaga and Ueda 2010; Halder and Ueda 2012). Interestingly, nuclear ProTα intensity was drastically increased in astrocytes by diminishing cytosolic contents, but not in microglia after the pre-treatment with Z-Val-Ala-Asp fluoromethyl ketone (Z-VAD-fmk), a caspase 3 inhibitor (Halder and Ueda 2012). The existence of caspase 3 activity in astrocytes in the adult brain as well as the caspase 3-mediated ProTα fragmentation *in vitro* has been reported previously (Enkemann *et al.* 2000; Evatafieva *et al.* 2003; Duran-Vilaregut *et al.* 2010; Matsunaga and Ueda 2010). Taken together, these studies suggested that caspase 3 controls the distribution of astroglial ProTα in the brain. However, the ischemia-induced ProTα release from brain is still under investigation. In the present study, we firstly attempted to see the cell type-specific non-classical release of ProTα as well as the effect of amlexanox on ProTα distribution in brain after cerebral ischemia.

Materials and methods

Middle cerebral artery occlusion mouse model

The transient middle cerebral artery occlusion (tMCAO) model was induced following the method as described previously (Egashira *et al.* 2004). Briefly, mice were anesthetized by 2% isoflurane (Mylan, Tokyo, Japan), and body temperature was monitored and maintained at 37°C during surgery. After a midline neck incision, the middle cerebral artery was occluded transiently using 8-0 in size monofilament nylon surgical suture (Natsume Co. Ltd., Tokyo, Japan) coated with silicon (Xantopren; Bayer dental, Osaka, Japan) that was inserted through the left common carotid artery and advanced into the left internal carotid artery. Following 1 h tMCAO, the animals were briefly re-anesthetized with isoflurane and the monofilament was withdrawn for reperfusion studies. As the silicon-coated nylon suture also plugs the branch from middle cerebral artery to supply blood to hippocampus in mice, due to small brain size, the ischemia-induced brain damages are also observed in the hippocampus. Cerebral blood flow was monitored by laser Doppler flowmeter (ALF21; Advance Co., Tokyo, Japan) using a probe (diameter 0.5 mm) of a laser Doppler flowmeter (ALF2100; Advance Co.) inserted into the left striatum (anterior: 20.5 mm; lateral: 1.8 mm from bregma; depth: 4.2 mm from the skull surface) through a guide cannula.

Drug treatment

Amlexanox (kindly provided by Takeda Pharmaceutical Company Ltd, Osaka, Japan) was dissolved in 0.05 N NaOH in phosphate buffered saline [K^+ free phosphate-buffered saline (PBS), pH 7.4], adjusted pH 7.6 by 0.1 M H_3PO_4, and finally diluted in PBS. Using Hamilton syringe, amlexanox was injected intracerebroventricularly (i.c.v.) at a dose of 10 μg/5 μL in the brain 30 min before ischemia. Vehicle was treated with equal volume of solution containing 0.05 N NaOH and 0.1 M H_3PO_4 in PBS 30 min before ischemia in a similar manner. However, Z-VAD-fmk was purchased from Sigma-Aldrich, St Louis, MO, USA and dissolved in dimethyl sulfoxide and finally diluted in artificial CSF. Z-VAD-fmk was delivered i.c.v. at a dose of 1 μg/5 μL in the brain 30 min before ischemia (1 h tMCAO). Following similar way, vehicle was treated with equal volume of artificial CSF in the brain 30 min before cerebral ischemia.

Cell counting

Measurements of ProTα- and S100A13-positive cells in the brain were done using the BZ Image Measurement software. Briefly, cell counts were carried out in bright field images following the protocol as reported previously (Matsumoto *et al.* 2006). The number of ProTα- and S100A13-positive neurons, astrocytes and microglia in the somatosensory cortex of brain were stereologically counted (bregma 0.62 to −2.06) in the square fields (approximately 250 μm × 250 μm) of vehicle-treated ($n = 3$) and amlexanox-treated ($n = 3$) ischemic brain and were normalized to those obtained identically in the control brain ($n = 4$). However, to determine the ProTα- and S100A13-positive cells, we carried out the counts using specific cell markers with clearly visible nuclei. The quantification was expressed as average percentage of the total number of cell type-specific ProTα- and S100A13-positive cells in the 4–7 brain sections per mouse.

Statistical analysis

All results are shown as means ± SEM. Two independent groups were compared using the Student's *t*-test. Multiple groups were compared using Dunnett's multiple comparison test after a one-factor ANOVA. $P < 0.01$ was considered significant.

Other methods

Animals, tissue preparations, antigen retrieval microwave technique and proteinase K treatment, and immunohistochemical analysis are available as Appendix S1.

Results

Cerebral ischemia-induced rapid depletion of ProTα from hippocampal neurons

Following cerebral ischemia (1 h tMCAO) in mice, we examined time-dependent changes in ProTα expression in the ipsilateral hippocampus throughout 1–24 h. The 3,3′-diaminobenzidine tetrahydrochloride immunostaining data revealed that ProTα depletion in ipsilateral CA1 pyramidal neurons starts as early as 1 h after the cerebral ischemia (Fig. 1b), completes at 3 h (Fig. 1c) and followed by a gradual recovery of ProTα signals through 24 h (Fig. 1–d–f). However, there were some cells showing intense ProTα-immunoreactivity in the ipsilateral stratum radiatum of hippocampus at 3 h (Fig. 1c). The ProTα signals in various cells in the stratum radiatum gradually increased as time goes thereafter (Fig. 1–d–f). However, there was no significant change in ProTα reactivity in the respective contralateral hippocampus of ischemic brain (Fig. 1–a–f). Similar results of ProTα depletion and recovery were also observed in the regions of striatum (Fig. 2–a–f) and somatosensory cortex (Fig. 2–g–l).

Ischemia-induced depletion of neuronal ProTα

To identify the cell type specificity for ProTα release after cerebral ischemia (1 h tMCAO) and reperfusion, coronal brain sections were co-stained with anti-ProTα IgG and antibody against Microtubule-associated protein (MAP-2), a cytoplasmic neuronal marker. Our double fluorescence immunohistochemical data explained that ProTα immunoreactivity is strictly localized in nuclei of MAP-2-positive CA1 pyramidal neurons of hippocampus in the control mice (Fig. 3a). In confocal microscopy observation, ProTα signals were also found in nuclei in the MAP-2-positive CA1 pyramidal neurons of control hippocampus (Fig. 3g). As early as 3 h after the cerebral ischemia and reperfusion, ProTα signals in CA1 pyramidal neurons were completely lost, whereas the signals were significantly enhanced in some non-neuronal cells in the stratum radiatum of hippocampus (Fig. 3b). ProTα in the nuclei of pyramidal neurons was recovered largely to the control levels, and the signals were also localized in the nuclei at 24 h (Fig. 3c). Like control, there was also no change in nuclear ProTα levels observed in the contralateral side of brain (data are not shown). Similar patterns of ProTα release at 3 h and recovery at 24 h were observed in MAP-2-positive neurons in the striatum (Fig. 3i) and somatosensory cortex (Fig. 3j and k) of ischemic brain.

Amlexanox-reversible blockade of neuronal ProTα release

To understand the phenomenon whether amlexanox blocks ischemia-induced non-classical release of ProTα *in vivo*, mice was treated with amlexanox (10 μg/5 μL; i.c.v.) 30 min before cerebral ischemia (1 h tMCAO). Our immunohistochemical results revealed that ProTα signals are completely lost in ipsilateral MAP-2-positive CA1 pyramidal neuronal cells in the hippocampus of PBS-pre–treated

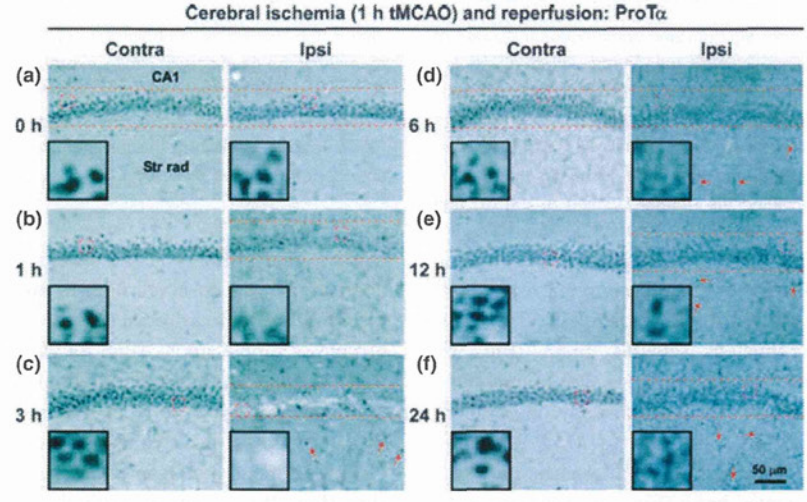

Fig. 1 Depletion of ProTα in the CA1 pyramidal cell layer of hippocampus under cerebral ischemia. (a–f) Immunostaining of ProTα in adult mice brain after ischemic stress. 3,3′-Diaminobenzidine tetrahydrochloride (DAB) immunostaining data of coronal brain sections indicate that ProTα is partially released at 1 h (b) followed by complete release at 3 h (c) in the ipsilateral CA1 pyramidal cell layer of hippocampus after ischemic stress (1 h tMCAO). Some cells show intense ProTα reactivity at 3 h in the stratum radiatum of hippocampus noted by arrow points (c). (d–f) ProTα level is recovered gradually in the ipsilateral CA1 pyramidal cell layer at the later time points that starts from 6 h (d) continuing 12 h (e) and 24 h (f) after ischemic stress. ProTα intensity is also gradually increased in the ipsilateral stratum radiatum of hippocampus through 24 h after ischemic stress noted by arrows (d–f). There is no change in ProTα staining at 0 h (a) as well as in the respective contralateral sides of hippocampus after ischemia. Insets in panels (a–f) indicate the higher magnification view of ProTα intensity noted by red squares.

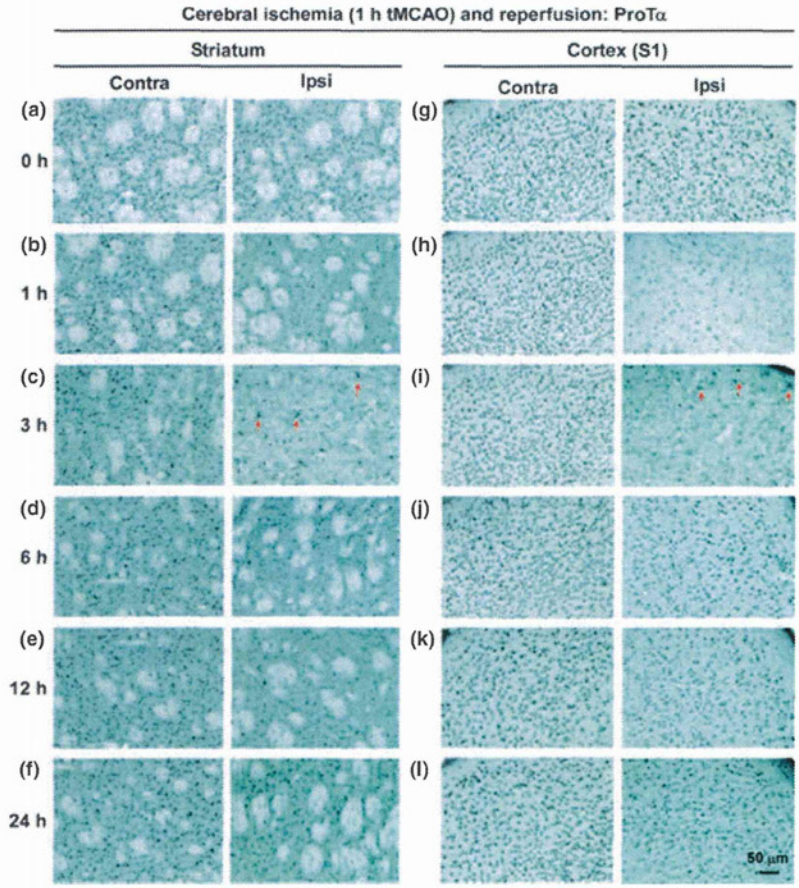

Fig. 2 ProTα is released from striatum and somatosensory cortex of ischemic brain. 3,3′-Diaminobenzidine tetrahydrochloride (DAB) immunostaining of coronal brain sections is performed using antibody against ProTα. (a–f) ProTα signal is partially lost at 1 h (b), followed by complete lost at 3 h (c) and recovery gradually at 6 h (d), 12 h (e) and 24 h (f) in the ipsilateral striatum after ischemic stress (1 h tMCAO) in adult mice, retaining the normal staining at 0 h (a) and also in the respective contralateral sides. (g–l) DAB immunostaining data show the time–course ProTα expression in the ipsilateral as well as contralateral somatosensory cortex of brain from 0 to 24 h after ischemic stress. (c, i) Some non-neuronal-like cells show intense ProTα reactivity at 3 h in the ipsilateral striatum (c) and somatosensory cortex (i) noted by arrows.

(vehicle) brain at 3 h after ischemia and reperfusion (Fig. 3d). However, ProTα was diffused to the cytoplasm from the nucleus in ipsilateral MAP-2-positive CA1 neurons in the amlexanox-pre–treated ischemic brain (Fig. 3e), preserving normal nuclear staining in the contralateral hippocampus (Fig. 3f). In confocal microscopy observation, we also found that ProTα is diffused to MAP-2-positive neuronal cytoplasm from nucleus at 3 h after ischemic stress in the amlexanox-pre–treated brain (Fig. 3h). Similar results were also observed in MAP-2-positive neuronal cells of ipsilateral striatum (Fig. 3i) and somatosensory cortex (Fig. 3j and k) in the ischemic brain.

Caspase 3 inhibition causes ProTα release from astrocytes

To investigate the clue whether ProTα is released from astrocytes *in vivo*, coronal brain sections were co-stained with anti-ProTα IgG and antibody against an astroglial marker, glial fibrillary acidic protein (GFAP). ProTα immunoreactivity was observed both in nucleus and cytoplasm in the GFAP-positive astrocytes located in the stratum radiatum of control hippocampus (Fig. 4a and g). In the presence of ischemic stress in brain, the findings clarified that the ProTα immunoreactivity is still observed with higher intensity in ipsilateral GFAP-positive astrocytes in the stratum radiatum of hippocampus at 3 h after cerebral ischemia and reperfusion (Fig. 4b), compared with the control brain (Fig. 4a). Indeed, the ProTα signals were increased gradually in astrocytes through 24 h (Fig. 4c). Similar results were also observed in astrocytes in the ipsilateral striatum (Fig. 4h) and somatosensory cortex (Fig. 4i and j) after ischemic stress in brain. Most recently, we demonstrated that ProTα is distributed in both cell body and cytosolic space of processes in adult astrocytes of mouse brain, and that ProTα signal in the astroglial nuclei is drastically increased by diminishing

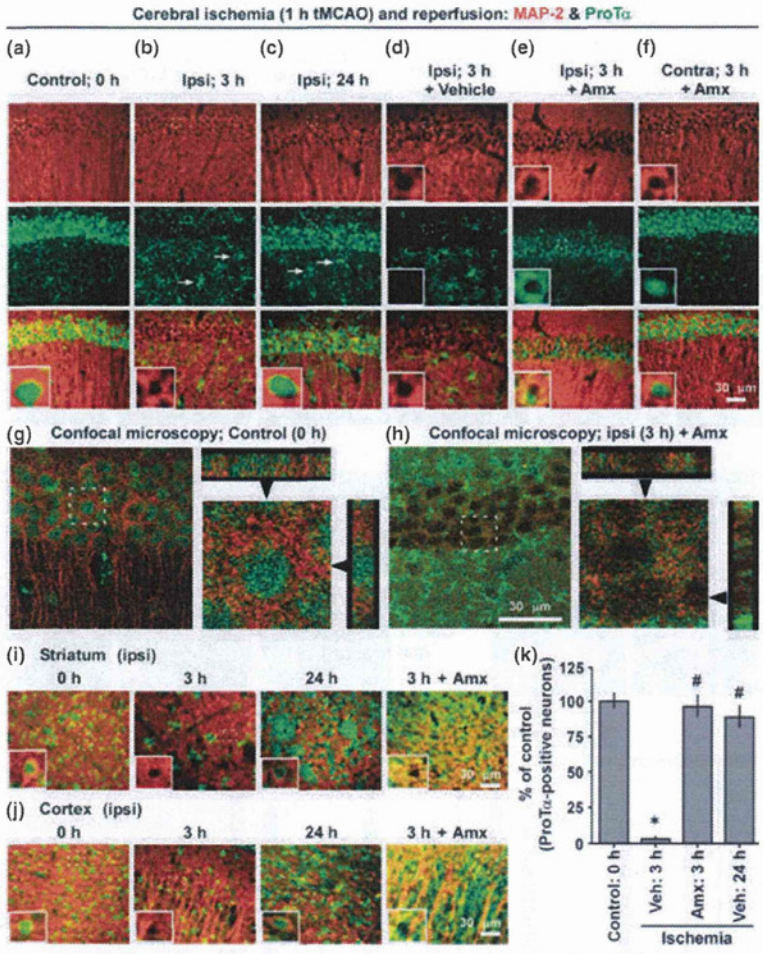

Fig. 3 Ischemia-induced ProTα depletion in neurons is blocked by amlexanox. Amlexanox (Amx) is injected (10 μg/5 μL; i.c.v.) in the mice brain 30 min before cerebral ischemia (1 h tMCAO). (a–j) Coronal brain sections are co-stained with antibodies against ProTα and MAP-2. (a, b) Double fluorescence immunostaining shows that ProTα signal is completely lost in MAP-2-positive neurons in the ipsilateral CA1 pyramidal cell layer of hippocampus (MAP-2, red; ProTα, green) at 3 h after cerebral ischemia (1 h tMCAO), compared with the nuclear ProTα staining in the MAP-2-positive neurons of control brain. (b) Some non-neuronal cells shows higher ProTα immunoreactivity in the ipsilateral stratum radiatum of hippocampus indicated at 3 h by arrow points. (c) ProTα is recovered in nuclei in the ipsilateral CA1 pyramidal neuronal cells at 24 h, but some non-neuronal cells shows the higher ProTα intensity in the stratum radiatum noted by arrows. (d) ProTα staining is completely lost in the ipsilateral MAP2-positive CA1 pyramidal neurons of PBS-pre–treated (vehicle) ischemic mice at 3 h. (e) Following Amx pre-treatment in ischemic mice brain, ProTα release is blocked in the ipsilateral MAP-2-positive CA1 pyramidal neurons and consequently translocated in the neuronal cytoplasmic spaces at 3 h after stress, compared with the contralateral side (f). (g, h) Conforcal microscopy observation indicates ProTα signals in the MAP-2-positive CA1 pyramidal neurons of hippocampus. A higher magnification view is indicated as doted square in (g) and (j), respectively. Arrowheads indicate the 3D imaged line (thickness: 10 μm), as shown in upper (*x*-axis) and right panels (*y*-axis). (i, j) Double fluorescence immunostaining shows that ProTα signal is completely lost in MAP-2-positive neurons in the ipsilateral striatum and somatosensory cortex at 3 h after 1 h tMCAO, compared with the normal nuclear ProTα staining in the control. ProTα signal is recovered in nuclei in the ipsilateral striatum and somatosensory cortex at 24 h after ischemia. Amx injection 30 min before ischemia inhibits the release of neuronal ProTα in the ipsilateral striatum and somatosensory cortex at 3 h after ischemic stress. Insets indicate the higher magnification view of ProTα localization in CA1 pyramidal neurons noted by dotted squares. (k) Quantitative analysis of ProTα -positive neurons in the somatosensory cortex. Data represent the means ± SEM ($^{*,\#}p < 0.01$, vs. the control: 0 h and the Amx: 3 h, respectively).

cytosolic levels when pre-treatment with Z-VAD-fmk, a caspase 3 inhibitor (Halder and Ueda 2012). In the present study, we confirmed that ProTα is also localized in both cell body and processes in immature astrocytes in the neonatal mice brain including stratum radiatum of hippocampus (Fig. 4k). Our *in vivo* experiments revealed that ProTα

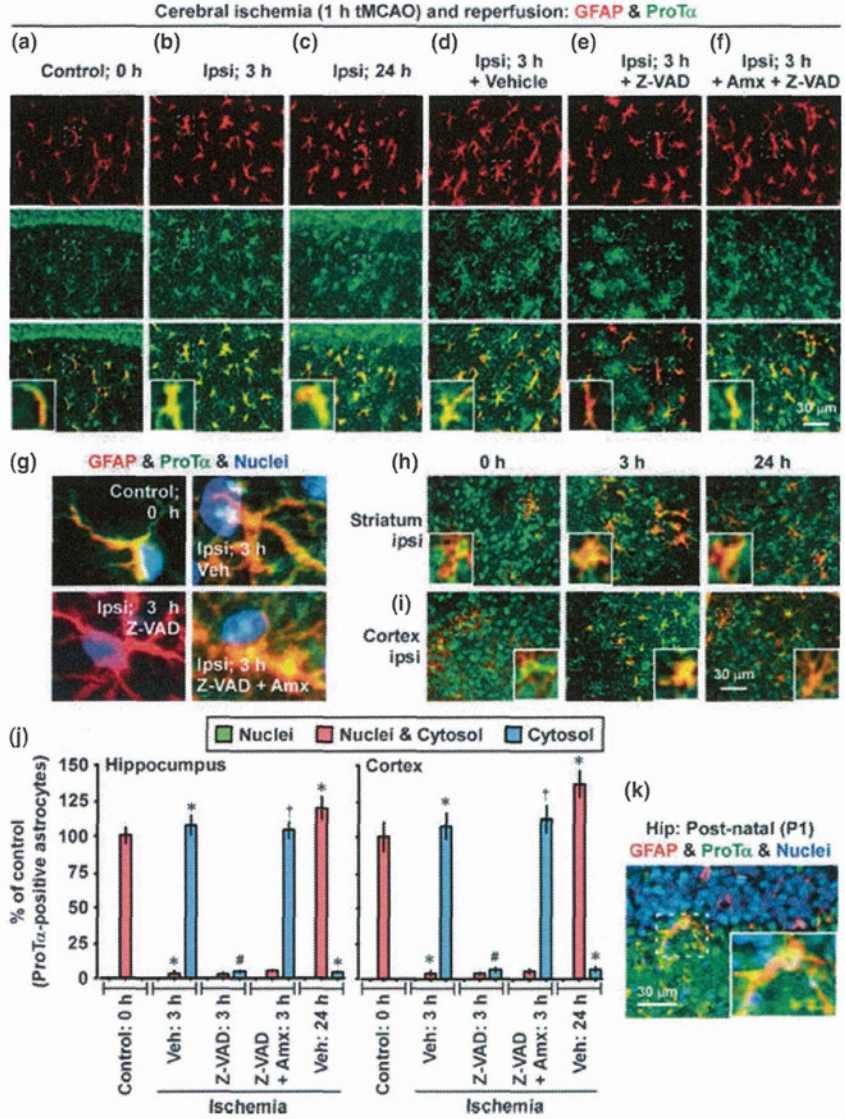

Fig. 4 Initiation of ProTα release from astrocytes by caspase 3 inhibition. Z-VAD-fmk (Z-VAD), a caspase 3 inhibitor (1 μg/5 μL) as well as Amx (1 μg/5 μL) is injected (i.c.v.) in the brain 30 min before cerebral ischemia (1 h tMCAO). Coronal brain sections are co-stained with antibodies against ProTα and GFAP. (a) Immunohistochemical analysis shows the expression of ProTα in GFAP-positive astrocytes in the stratum radiatum of hippocampus in control brain (GFAP, red; ProTα, green). (b) Higher ProTα signal is found in GFAP-positive astrocytes in the ipsilateral stratum radiatum at 3 h after ischemia. (c) The signal is gradually increased in astrocytes through 24 h after ischemia. (d) Intense ProTα signal is observed in GFAP-positive astrocytes in the ipsilateral stratum radiatum at 3 h after ischemia in the in PBS-pre-treated (vehicle) mice. (e) Following Z-VAD-fmk pre-treatment and ischemic stress, ProTα signal is significantly decreased in GFAP-positive astrocytes in the ipsilateral stratum radiatum at 3 h. (f) Z-VAD-fmk-induced ProTα release is blocked from GFAP-positive astrocytes in the ipsilateral stratum radiatum at 3 h after ischemia in Amx pre-treated brain. (g) Higher magnification views of ProTα in astrocytes in the control brain (upper left panel), the vehicle pre-treated ischemic brain (upper right panel), the Z-VAD-fmk pre-treated ischemic brain (lower left panel), and Amx + Z-VAD-fmk pre-treated ischemic brain (lower right panel) at 3 h after stress. (h, i) ProTα is not released from astrocytes in the striatum and somatosensory cortex after cerebral ischemia. ProTα signal is found with higher intensity in GFAP-positive astrocytes in the ipsilateral striatum and somatosensory cortex at 3 h after ischemic stress, compared with the ProTα signals in the control brain. ProTα intensity is gradually increased in GFAP-positive astrocytes in the ipsilateral striatum and somatosensory cortex through 24 h after ischemic stress. (j) Quantitative analysis of ProTα localization of astrocytes in the stratum radiatum of hippocampus (left panel) and somatosensory cortex (right panel). Data represent the means ± SEM. ($^{*,\#,\dagger}P < 0.01$, vs. the control: 0 h, the Veh: 3 h, and the Z-VAD: 3 h, respectively). (k) ProTα is localized both in cell body and processes in the astrocytes of post-natal (P1) mice brain (GFAP, red; ProTα, green; Nuclei, blue). Insets indicate the higher magnification view of ProTα expression in astrocytes noted by dotted squares.

signal is significantly lost in mature astrocytes in the stratum radiatum of hippocampus as early as 3 h after cerebral ischemic stress in adult mice brain pre-treated with Z-VAD-fmk (Fig. 4e and g), whereas higher reactivity was observed in astrocytes in the PBS-pre–treated (vehicle) ischemic brain (Fig. 4d and g), an indication of ProTα release from astrocytes. Following the combined pre-treatment with Z-VAD-fmk, amlexanox and subsequent ischemia, the signals in astrocytes were recovered as the level in vehicle at 3 h, indicates that Z-VAD-fmk-induced ProTα release from astroglia is blocked by amlexanox (Fig. 4f and g). We also found the similar effects of Z-VAD-fmk and amlexanox on GFAP-positive astroglial ProTα in the ipsilateral the striatum (data are not shown) and somatosensory cortex (Fig. 4j).

No ProTα release from microglia

To see cerebral ischemia-induced ProTα expression in microglia, coronal brain sections were co-stained with anti-ProTα IgG and antibody against Iba-1 (a microglia marker). Recently, we reported that ProTα is localized in both cell body and cytosolic space of processes in microglial in the adult mice brain (Halder and Ueda 2012). Our immunohistochemical analysis suggested that ProTα is also distributed in whole cell in microglia in the adult and neonatal mice brain (Fig. 5a and f). Using the adult brain, the ProTα reactivity was still observed with higher intensity in Iba-1-positive microglia in the ipsilateral stratum radiatum of hippocampus as early as 3 h after ischemia (1 h tMCAO) and reperfusion (Fig. 5b), compared with the control brain (Fig. 5a). However, the ProTα signals were increased gradually in microglia through 24 h (Fig. 5c). On the other hand, there was no effect on microglial ProTα levels by pre-treatment with Z-VAD-fmk in ischemic brain (Fig. 5e), compared with the intensity in the PBS-pre–treated (vehicle) ischemic brain (Fig. 5d). Similar results of ischemia-induced ProTα expression in Iba-1-positive adult microglia were also observed at 3 h and 24 h after ischemia in the regions of striatum (Fig. 5g) and somatosensory cortex (Fig. 5h and i), the regions from where the ProTα signals were completely lost in neurons.

Neuronal depletion of S100A13, a cargo protein for non-classical release

Recently, *in vitro* experiments demonstrated that the non-classical release of ProTα requires interaction with C-terminal sequence of S100A13, a cargo protein (Matsunaga and Ueda 2010). To examine the phenomenon whether S100A13 is released from neurons of adult brain under cerebral ischemic stress (1 h tMCAO), coronal brain sections were co-stained with anti-S100A13 and anti-NeuN antibodies. Our immunostaining data revealed that S100A13 is expressed in NeuN-positive neurons in the CA1 pyramidal cell layer of hippocampus (Fig. 6a), and also in neurons in the striatum (Fig. 6i) and somatosensory cortex (Fig. 6j) of mice brain. As early as 3 h after ischemia and reperfusion, S100A13 was released completely from ipsilateral NeuN-positive CA1 pyramidal neurons (Fig. 6b), compared with the control (Fig. 6a). However, the dot-like signals were observed in some non-neuronal cells in the stratum radiatum of hippocampus (Fig. 6b). S100A13 in pyramidal neurons was recovered in a lesser level at 24 h after ischemia, whereas non-neuronal cells in stratum radiatum completely released S100A13 at this time point (Fig. 6c). Similar results of S100A13 release were observed in ipsilateral neurons of striatum (Fig. 6i) and somatosensory cortex at 3 h (Fig. 6j and k) as well as recovery in neurons at 24 h (Fig 6k) after cerebral ischemic stress.

Blockade of neuronal S100A13 release by amlexanox

It has been described previously that the non-classical release of S100A13 from C6 glioma cells is blocked by amlexanox upon serum-deprivation stress (Matsunaga and Ueda 2010). To investigate the *in vivo* effect of amlexanox on the stress-induced non-classical release of S100A13 from adult brain, mice were treated with amlexanox (10 μg/5 μL; i.c.v.) 30 min before cerebral ischemia (1 h tMCAO) and reperfusion. Using anti-S100A13 and anti-NeuN antibodies, our immunohistochemical findings suggested that S100A13 signals are completely lost in ipsilateral NeuN-positive neurons in the CA1 pyramidal cell layer of hippocampus at 3 h after ischemia in PBS-pre–treated (vehicle) brain (Fig. 6e), retaining the normal staining in the control brain (Fig. 6d). Whereas, S100A13 reactivity was rescued in ipsilateral NeuN-positive CA1 neurons in the ischemic brain pre-treated with amlexanox, an indicative of non-classical blockade of neuronal S100A13 release by amlexanox (Fig. 6f). In confocal microscopy observation, we found that S100A13 immunoreactivity was increased in NeuN-positive CA1 pyramidal neurons of hippocampus due to the blockade of its release by amlexanox (Fig. 6h), compared with the control (Fig. 6g). This result suggests that ischemic stress might cause the up-regulation of S100A13, as shown in Fig. 6c. We also observed the similar results of amlexanox effect on the release of neuronal S100A13 in the striatum (Fig. 6i) and somatosensory cortex (Fig. 6j and k) after the onset of cerebral ischemic stress.

S100A13 is released from astrocytes, but not from microglia

To find out whether S100A13 is released from non-neuronal astrocytes and microglia in the adult brain under cerebral ischemic stress (1 h tMCAO), coronal brain sections were co-stained with anti-S100A13 and antibodies against GFAP and Iba-1. Our double immunostaining data showed that S100A13 is expressed in GFAP-positive astrocytes in the adult mice brain including stratum radiatum of hippocampus (Fig. 7a and c). Following cerebral ischemia and reperfusion, S100A13 signals were partially lost at 3 h in the GFAP-